universität wien

MASTERARBEIT / MASTER'S THESIS

Titel der Masterarbeit / Title of the Master's Thesis

„Novel FimH peptide analogs as targeting ligands in the intravesical treatment of bladder diseases“

verfasst von / submitted by

Hatixhe Sahini, BSc

angestrebter akademischer Grad / in partial fulfilment of the requirements for the degree of

Magistra pharmaciae (Mag.pharm.)

Wien, 2024 / Vienna, 2024

Studienkennzahl lt. Studienblatt / degree programme code as it appears on the student record sheet:	UA 066 605
Studienrichtung lt. Studienblatt / degree programme as it appears on the student record sheet:	Masterstudium Pharmazie
Betreut von / Supervisor:	ao. Univ.-Prof. Mag. Dr. Michael Wirth

Danksagungen

An dieser Stelle möchte ich mich bei allen herzlich bedanken, die mich im Laufe der Anfertigung dieser Masterarbeit unterstützt haben.

Zuerst möchte ich mich bei ao. Univ.-Prof. Mag. Dr. Michael Wirth und ao. Univ.-Prof. Mag. Dr. Franz Gabor bedanken, die es mir ermöglicht haben Teil Ihrer Forschungsgruppe zu werden und für die besonders herzliche Aufnahme in die Arbeitsgruppe. Besonderer Dank gilt ao. Univ.-Prof. Mag. Dr. Michael Wirth für die umfassende Betreuung, die Unterstützung und die Möglichkeit an diesem spannenden Thema zu arbeiten.

Ein großes Dankeschön möchte in an dieser Stelle auch an Mag. Dr. Katharina Skoll aussprechen, die mir zu jeder Zeit mit Rat, Hilfestellungen und Ideen beistand und mich immer mit ihrer Begeisterung motiviert hat.

Zudem möchte ich mich herzlich bei Ass.-Prof. Dr. Ulrich Lächelt bedanken für die hilfreichen Anregungen und Tipps, die mir im Laboralltag sehr geholfen haben.

Außerdem möchte ich mich bei der ganzen Arbeitsgruppe bedanken, für ihre Hilfe aber auch für ihre herzliche Art und die schöne gemeinsame Zeit.

Mein besonderer Dank gilt meiner Familie, insbesondere meinen Eltern, meinen Brüdern und meinem Freund die mich immer bei jeder Entscheidung unterstützt haben, mich motiviert haben und immer an mich geglaubt haben. Ohne euch wäre das alles nicht möglich gewesen.

Abstract

Pathologic conditions of the urinary bladder, such as bladder cancer or urinary tract infections, often exhibit high reoccurrence rates making their treatment more difficult. Direct bladder instillation presents a promising application route to enhance the drug delivery to the affected site. Nonetheless, direct instillation has several limitations such as drug dilution by urine production and inaccessibility due to the highly effective barrier function of the bladder. Thus, effective treatment of bladder cancer and urinary tract infections often remains unattainable.

The present master thesis aimed to investigate new peptide molecules to prolong the persistence time of drugs in the urinary bladder and thus potentially enhancing drug delivery. Therefore, peptides similar to the binding domain of FimH of the bacterial E. coli, which exhibits a high affinity to the urothelium, were synthesized, characterized, and tested concerning their cell-associative properties on healthy and cancerous bladder cells.

The investigated peptides exhibited cell-adhesive properties for both cancerous and healthy bladder cells. Especially to cancerous bladder cells the peptides showed a significantly enhanced cell adherence. Furthermore, fluorescence microscopic analysis revealed that the peptides showed not only binding to the cell surface but also internalization into cancerous bladder cells.

This study might represent a first step towards a novel targeting ligand to overcome the limitations of intravesical therapy of the human urinary bladder.

Contents

1 Introduction

1.1 Bladder cancer and urinary tract infections

Bladder cancer and urinary tract infections (UTIs) are two diseases of the urinary bladder that have a major influence on many patients worldwide. (1)

Bladder cancer represents a significant global health problem being the tenth most common cancer worldwide in 2018, with a greater prevalence in men than women. (2) The cancer stage and treatment are determined by the degree of penetration and invasiveness of the cancer. (1, 3) 70% of new cancer diagnoses pertain to non muscle-invasive bladder cancers (NMIBCs). Muscle-invasive bladder cancers (MIBCs) invade muscle tissue and are more likely to generate metastases making their treatment more difficult. (3) Generally, the treatment of urothelial cancer consists of resection of the tumor followed by intravesical chemotherapy. (1) UTIs on the other hand, are bacterial infections that can range from mild to life-threatening conditions with high reoccurrence rates. These infections are especially common in women and are caused predominantly by bacterial uropathogenic Escherichia coli (UPEC). UTIs can be classified as uncomplicated and complicated cystitis, respectively. Untreated infections can lead to severe infections of the kidneys and further to life-threatening sepsis when the pathogens get into the bloodstream. In most cases, UTIs are treated with orally administered antibiotics. (4)

1.2 Limitations in the treatment of bladder diseases

Despite the development of different therapy strategies, recurrences in both conditions remain a problem. When treating bladder diseases with systemically administered drugs only a fraction of the drug reaches the affected site. Therefore, higher doses are required and systemic adverse side effects occur more frequently. (1) Furthermore, due to the rapidly growing problem of drug resistance among pathogens and further disruption of homeostasis of the host microbiome, caused by long-term systematic antibiotic administration, there is a growing need for a target site antibiotic therapy. (4, 5)

As an alternative drugs can be administered by the intravesical route, presenting high drug concentrations directly at the affected site. (1, 5) In the follow-up treatment of bladder cancer intravesical administration is already indispensable, with drugs being directly instilled into the urinary bladder. (1) In complicated UTIs intravesical therapy presents a potential alternative application route compared to oral administration of antibiotics. By intravesical application of an active pharmaceutical ingredient (API) a higher dosage could be applied to the diseased tissue, efficacy raised and side effects and the probability of antibiotic resistance could be reduced. (4, 5)
However, intravesical instillation has its limitations. Drugs instilled into the bladder are washed out by urine production, thus limiting the drugs' persistence time. Therefore, a more frequent application of the drug is needed. Moreover, due to the highly effective barrier function of the bladder epithelium drugs show low permeability in the urothelium. (1)

These limitations could be overcome by extending the persistence time of drugs in the bladder by a targeted drug delivery system. An example of specific targeting of the urinary bladder was investigated with the plant lectin wheat germ agglutinin (WGA) which was shown to have cytoadhesive and cytoinvasive properties on urothelial cells. (6) Furthermore, surface modification of PLGA nanoparticles (7-9) and HSA nanoparticles with WGA (10, 11) improved cell-associative properties of nanoformulations on urothelial cells.

1.3 Type 1 fimbrial lectin FimH

Lectins are carbohydrate-binding proteins that are found in many living organisms such as plants (e.g., WGA), animals, or bacteria. (12) Bacteria utilize lectins to adhere to cell surfaces, a process facilitated by expressing cell surface organelles called “fimbriae” or “pili”. (13) These fimbriae have lectin units that interact non-covalently, highly specific, and usually reversibly with carbohydrates via a carbohydrate recognition domain (CDR). (12, 13)

Approximately 90% of uropathogenic E. coli express type 1 pili on their surface with the bacterial FimH lectin at the distal tip. (13, 14) By specifically targeting α-D-mannose residues the type 1 fimbrial lectin FimH enables UPEC to adhere efficiently to the urothelium. In more detail, FimH was observed to target mannosylated glycoproteins (15) such as uroplakins Ia

and Ib with high mannose-type sugar found on the apical surface of the urothelial epithelium. (15, 16) Furthermore, FimH was shown to induce programmed cell death, exfoliation of bladder epithelium cells, and invasion into deeper tissue playing an important role in the pathogenic colonization and persistence of E. coli in the urinary tract. (17, 18)

The crystal structure of FimH adhesin was resolved in complex with FimC chaperone (Choudhury et al., 1999) and as the FimC-FimH chaperone-adhesin complex with α-D-mannose (Hung et al., 2002). (14, 18)

FimH consists of 279 amino acid residues and two domains: the N-terminal receptor binding domain consists of the residues Phe1 to Thr156, and the C-terminal pilin domain comprises the residues 160 to 279. At the tip of the receptor binding domain of FimH the binding pocket for α-D-mannose is located. (14, 18) Within a negatively charged pocket a single α-D-mannose molecule is buried, offering a generous surface for tight engagement between the binding pocket and the sugar. (18)

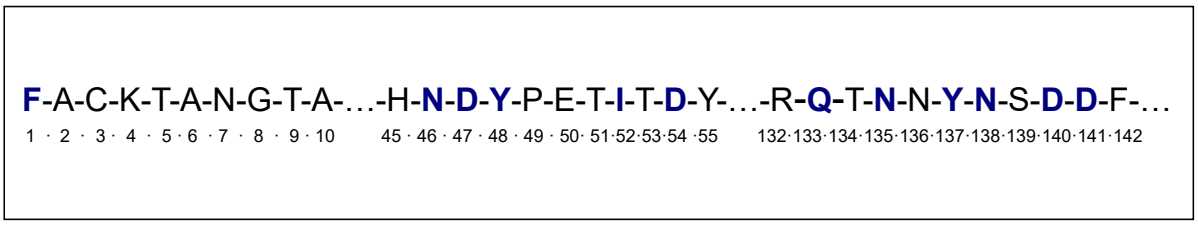

Figure 1: FimH analogs primary sequence of the residues 1-10, 45-55, and 132-142 in the one-letter code, respectively

The residues that mold the carbohydrate-binding pocket of FimH are displayed in bold and colored in blue. Residue Ile13 which also lines the carbohydrate-binding pocket is not illustrated in this figure. (14) (created with ChemDraw)

Figure 1 illustrates a part of the primary sequence with the residues Phe1, Ile13, Asn46, Asp47, Tyr48, Ile52, Asp54, Gln133, Asn135, Tyr137, Asn138, Asp140, Asp141 that line the surface of the carbohydrate-binding pocket of FimH. (14)

In the binding pocket all hydroxyl groups of α-D-mannose, excluding O1, interact with the binding pocket to a great extent. Asn46, Asp47, Asp54, Gln133, Asn135, Asp140, and Phe142 of FimH engage with the α-D-mannose molecule via hydrogen bonds and hydrophobic interactions. Additionally, the N-terminal group interacts with the oxygen atoms of the mannose. O2 also interacts with the water molecule inside the binding pocket. Furthermore,

the pocket is stabilized by the stacking of the aromatic ring of Phe1, the side chain of Gln133 and Phe144. Moreover, a hydrophobic ridge surrounds the binding pocket comprising the amino acids Ile13, Tyr48, Ile52, and Phe142. Its function may be to increase the affinity to α-D-mannose by leading the mannose molecule to the binding pocket. (18)

1.4 Aim of the thesis

The present master thesis aimed to develop peptides with a high affinity to cancerous and healthy human bladder cells that mimic the bacterial lectin FimH to prolong the persistence time of drugs in the urinary bladder.

Three peptide analogs containing the residues of the primary sequence of bacterial lectin FimH that form the carbohydrate-binding pocket were synthesized and characterized. Specifically, peptides comprising the residues 1-10, 45-55, and 132-142, respectively, of the FimH primary sequence were synthesized along with their control peptides that contained a random primary sequence (see Figure 1 for the primary sequence of FimH and 3.1 “Characterization of the synthesized peptides”).

To investigate the cell-adhesive and cytoinvasive properties of the peptides, cell assays with healthy and cancerous bladder cells were performed using flow cytometry and fluorescence microscopic analysis.

2 Methods and Materials

2.1 Used materials

All Fmoc-protected amino acids (see Appendix 1 for a complete listing of all the used amino acids), dimethylformamide (DMF), 2-(1H-Benzotriazole-1-yl)-1,1,3,3-tetramethyluronium hexafluorophosphate (HBTU) and piperidine (peptide grade) were obtained from Iris Biotech GmbH (Marktredwitz, Germany). The Tentagel S Ram resin was acquired from Rapp Polymere GmbH (Tübingen, Germany).

1-Hydroxybenzotriazole hydrate (HOBt hydrate), acetic anhydride, acetonitrile, D-(+)-galactose, D-(+)-mannose, dimethyl sulfoxide (DMSO), di-*tert*-butyl dicarbonate, dichloromethane (DCM), ethyl cyano(hydroxyamino)acetate (oxyma), fluorescein-5-isothiocyanate (FITC), Gibco™ F12K Nutrient Mixture (Kaighn's Modification) 500 ml, hydrazine hydrate, magnesium chloride hexahydrate, *N*-hexane, *N,N*-diisopropylcarbodiimide (DIC), *N,N*-diisopropylethylamine (DIPEA), ninhydrin, paraformaldehyde, potassium cyanide, pyridine, RPMI 1640 medium powder, sodium phosphate dibasic dihydrate, *tert*-butyl methyl ether (MTBE), trifluoroacetic acid (TFA) and triisopropylsilane (TIPS) were obtained from Sigma Aldrich (Darmstadt Germany). Acetonitrile, methanol, and potassium chloride were purchased from Honeywell Riedel-de-Haën (Seelze, Germany), and ammonium chloride, ethanol, and potassium dihydrogen phosphate from Merck (Darmstadt, Germany). Calcium chloride dihydrate, gentamicin sulfate, 4-(2-Hydroxyethyl)-1-piperazine ethanesulfonic acid (HEPES), L-glutamine, phenol, sodium chloride, sodium bicarbonate were acquired from Carl Roth GmbH + Co. KG (Karlsruhe, Germany). HOECHST 33342 and Alexa Fluor® 594-labeled WGA (aWGA) were from Invitrogen (Paisley, United Kingdom), IsoFLOW Sheath Fluid from Beckman Coulter, Inc. (Brea, CA, USA), UV-Cuvettes micro (12,5 x 12,5 x 45 mm) from Brand GmbH + Co. KG (Wertheim, Germany), 96 well plates (PS, F-bottom, clear, sterile) from Greiner Bio-One International GmbH (Frickenhausen, Germany) and fetal bovine serum (FCS) from Corning (Corning, NY, USA).

2.2 Used buffers, mediums, and solutions

All buffers and mediums were prepared by dissolving and mixing the instructed components and following sterile filtration with a filter unit of 0.2 µm pore size.

Used buffers and mediums	
PBS buffer with Ca^{2+} and Mg^{2+} pH 7.04 0.003 M	0.1335 g $CaCl_2$* $2H_2O$ was dissolved in 50 ml distilled water. 0.2g KCl + 0.2g KH_2PO_4 + 0.1g $MgCl_2$*$6H_2O$+ 8g NaCl + 0.764g Na_2HPO_4 * $2H_2O$ were dissolved in 950 ml distilled water, then combined with the $CaCl_2$ solution and the pH was adjusted to 7.04 with 0.1 M HCl using a pH meter Seven compact (Mettler-Toledo GmbH, Vienna, Austria).
Isotone HEPES pH 7.4	4.77 g HEPES + 8 g NaCl were dissolved in 1 l distilled water and adjusted to pH 7.4 with 4M NaOH using a pH meter Seven compact (Mettler-Toledo GmbH, Vienna, Austria).
F12K medium	1 L F12 K Nutrient Mixture (2 x 500 ml) + 100 ml FCS + 10 ml Penstrep + 400 µl L-glutamine (c= 200 mM).
Roswell Park Memorial Institute (RPMI) – 1640 medium	One flask of RPMI 1640 medium powder was dissolved in 800 ml distilled water, adjusted to pH 4 with 4M HCl to accelerate the dissolving process. Then the pH was adjusted to approximately 7.2, before adding 2 g $NaHCO_3$. Finally, the pH value was set at 7 and 400 µl of L-glutamine solution (c=200 mM), 2 ml of gentamicin solution (c=110.01 mg/ml), 100 ml FCS and 200 ml distilled water were added.

2.3 Peptide synthesis

The synthesis of the peptides was based on solid-phase peptide synthesis (SPPS). SPPS has various benefits such as the minimization of loss of products through physical insoluble support and the removal of byproducts and reagents by simple washing steps. On the other hand, this method also has its limitations stemming from possible incomplete reactions and resulting byproducts which can affect the purity of the peptide.

The concept of the chosen Fmoc-method is based on using L-amino acids with base-labile Fmoc-protected α-amino groups and base-stabile, but acid-labile side chain protective groups. The basic steps of deprotection, followed by a Kaiser Test, coupling of another amino acid, and confirmation of successful coupling via a Kaiser Test are repeated until the desired peptide is finished. This way a directed synthesis from the C-terminal to the N-terminal α -amino end is possible. (19) The basic principle of the synthesis is visualized in the following Figure 2:

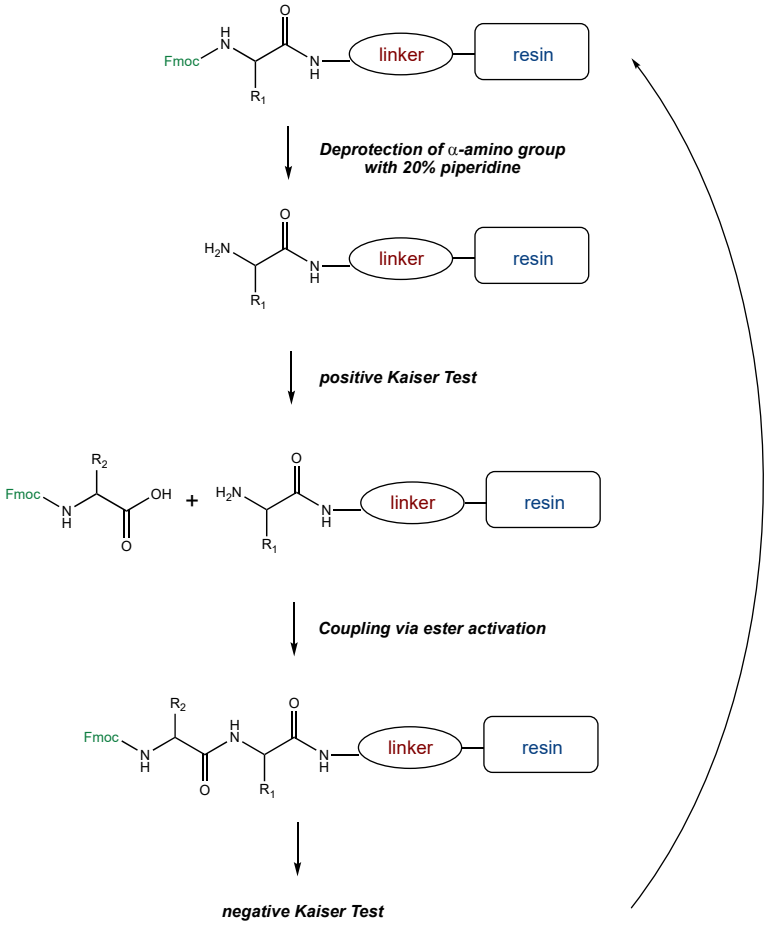

Figure 2: Basic principles of Fmoc-based peptide synthesis (created by ChemDraw)

The amino acid was attached to the linker molecule via its carboxy function. For peptide elongation in the direction of the α-amino-terminal group the deprotection of the Fmoc-protected α-amino group was conducted using 20% (v/v) piperidine in DMF. The protecting groups of the side chains of amino acids remained intact throughout the synthesis conditions.

To confirm that the deprotection was successful a Kaiser Test was performed. The Kaiser Test is based on the Ninhydrin reaction and is a qualitative test for the absence or presence of primary amino groups. In the case of the presence of a primary amino group, meaning completed deprotection of the α-amino group, the test shows a positive, dark blue color. A negative test where the beads remain colorless indicates that the deprotection is not completed. Practically, a Kaiser-Test was performed by adding one drop of 5% (m/V) ninhydrin solution in ethanol, 80% (m/V) phenol solution in ethanol, and a 20 µM KCN solution in pyridine to a few resin beads. To start the underlying ninhydrin reaction the sample was shaken for 4 minutes at 99 °C using an Eppendorf Thermomixer® compact (Eppendorf SE, Hamburg, Germany). It must be noted that proline which has a secondary amino group on the α-end shows no positive result.

The next amino acid was coupled in 4-fold excess to the chosen peptide scale. To ensure an efficient coupling, the activation of the carboxy function is needed which was performed by in-situ ester formation. The generated ester then reacts with the α-amino group of the previous amino acid forming an amide bond between two amino acids.

During manual peptide synthesis HBTU, DIPEA, and HOBt were used for the in-situ ester formation. HBTU is used as a coupling agent which converts the carboxy function of the Fmoc-amino acid to the corresponding OBt ester, specifically a benzotriazole-ester, in the presence of the tertiary base DIPEA. As an additive HOBt suppresses the enantiomerization. (19)

In the automatic peptide synthesizer *N,N*-diisopropylcarbodiimide (DIC) was used as the coupling agent while oxyma acted as an additive for better yield and less racemization. The carboxy function of the amino acid reacts with the carbodiimide to the highly reactive O-acylisourea intermediate. Adding oxyma as an additive leads to the formation of a less but still reactive ester, thus minimizing racemization. (20)

In the executed experiments a Tentagel S RAM resin with a modified rink amide linker was chosen. The linker forms a stable but reversible linkage between the solid resin and the growing peptide throughout the synthesis conditions, and further protects the C-terminal group. The linker as well as the side chain protecting groups have TFA-labile properties. After finished synthesis this linker yields a peptide with an amide function on the C-terminal group after acidolysis with TFA. (19) A visual representation of the rink amide linker is presented in the following figure 3: (21)

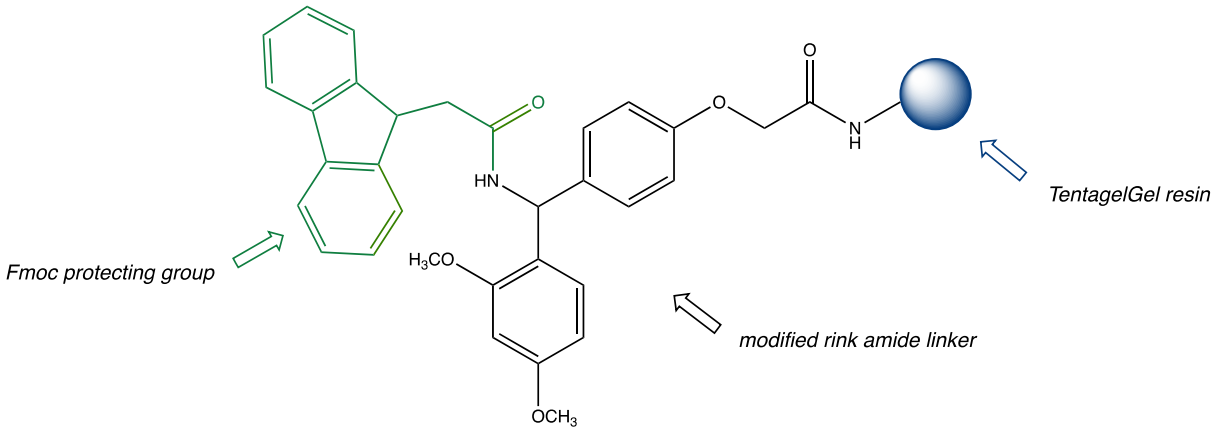

Figure 3: TentaGel S RAM resin with modified Rink amide linker (created with ChemDraw)

After successful coupling the next cycle was repeated until the desired peptide was completed. To study cell interaction between peptides and single human bladder cells, fluorescent labeling was done before yielding the finished product. For this purpose, every peptide contained an additional C-terminal amino acid L-Lys-(Dde)-OH which acted as the anchor point for the fluorescent dye FITC.

As the modified rink amide linker and protecting side chain groups are acid labile, the peptide is obtained with a cleavage cocktail consisting of trifluoroacetic acid (TFA), water, and triisopropylsilane (TIS). TIS is used as a cation scavenger during side chain deprotection with TFA, as protecting groups form stable cations during side chain deprotection with TFA. TIS irreversibly donates a hydride to the resulting cation, thus driving the equilibrium towards the cleavage of the side chain protecting groups. (22) After precipitation, purification, and identification of its structure the peptides were used in cell experiments.

The used peptides were obtained by manual peptide synthesis as well as an automatic peptide synthesizer. The peptides mimicking crucial FimH binding sites were synthesized by Peptide Synthesizer Liberty Blue™ 2.0 (CEM Corporation, Matthews, NC, USA). The control peptides which consisted of a randomized primary sequence of the peptides (generated by "random.org") were synthesized manually by solid-phase peptide synthesis. In both cases further modification steps, including the labeling with the fluorescent dye FITC and cleaving of the peptide, were performed manually. All following descriptions were executed for each peptide individually.

2.3.1 Synthesis by peptide synthesizer

The sequences detrimental to FimH-binding were synthesized by an automatic peptide synthesizer Liberty Blue™ using a Tentagel S RAM resin at a 100 µmol peptide scale and a resin-loading of 0.23 mmol/g, respectively. The automatic synthesizer was kindly provided by Prof. Manfred Ogris and Mag. Dr. Simon Decker (University of Vienna, Austria) kindly helped us with the handling of the peptide synthesizer. The first amino acid Fmoc-Lys-(Dde)-OH (4 eq, 213.1 mg) was coupled by hand (as described in the following chapter 2.3.2 "manual SPPS"), to continue the rest of the synthesis on the automatic device. In preparation for the latter, all amino acids (4 eq) were weighed into separate tubes and dissolved in DMF to prepare 0.2 M solutions, while the resin (434.78 mg) was suspended in a 1:1 DMF:DCM mixture. To activate the carboxy function DIC (1 M, 3 g) was used in combination with oxyma (1 M, 3.55 g) creating a reactive in-situ ester. After completing synthesis, the peptide underwent modification and cleavage as described under the subpoint 2.3.3 "Peptide modification".

2.3.2 Manual SPPS

The manual synthesis was carried out on a Tentagel S RAM resin at a 40 µmol peptide scale and 0.23 mmol/g resin loading. The synthesis conditions were set as follows: the synthesis was started by swelling the resin (173.91 mg) in DCM for 30 minutes under continuous movement and following incubation with a 20% (V/V) piperidine solution in DMF for Fmoc-deprotection of the linker. Between deprotection and incubation steps the resin was washed thoroughly with DMF followed by DCM, repeating each washing step three times. To ensure

successful deprotection a Kaiser test was performed. For every peptide the amino acid Fmoc-L-Lys-(Dde)-OH (4 eq, 85.2 mg) was coupled to the resin as the first amino acid.

Every coupling step, including the first amino acid, was operated in the same manner: amino acid (4 eq), HBTU (4 eq, 60.7 mg), and HOBt (4 eq, 24.6 mg) were each weighed separately. Subsequently, HBTU and then HOBT were dissolved in DMF (2.5 ml / g resin, 437.5 µl) whereas the amino acid was dissolved in DCM (2.5 ml / g resin, 437.5 µl) and DIPEA (8 eq, 55.8 µl) was added. Both solutions were combined, added to the resin, and incubated under constant movement and room temperature for 60 minutes. Afterwards, washing steps were repeated as described previously. Efficient coupling was verified by a negative Kaiser Test. Following the removal of the Fmoc group with 20% (v/v) piperidine in DMF, the deprotection efficiency was confirmed with a positive Kaiser Test, and a new coupling cycle was started. These steps were repeated until the desired peptide was achieved.

2.3.3 Peptide modification

After successful peptide synthesis, either by manual SPPS or Liberty Blue™ 2.0, the peptide was further modified. In both cases a 20 µmol peptide scale (86.96 mg resin) was chosen for the modification. As the peptide coupled to the resin had a terminal deprotected amino group, di-*tert* butyl dicarbonate (boc-anhydride) (4 eq, 17.46 mg) was weighed in a tube, and dissolved in 500 µl DCM before DIPEA (8 eq, 27.35 µl) was added. The pre-swelled resin was incubated with the described solution under continuous movement for one hour at room temperature. After the protection step the resin was washed thoroughly with DMF and DCM. At this point all amino groups were protected which was approved by a negative Kaiser Test.

To ensure the fluorescence labeling at the lysine side chain, an amino acid with a hydrazine-labile protecting group was chosen. Subsequently, the protecting group on the L-lysine side chain was removed by incubating with a freshly prepared 2% (V/V) hydrazine solution in DMF. The incubation step was repeated 15 times for three minutes each. Afterwards, the efficient deprotection was confirmed by a Kaiser Test. As an additional control, the amount of cleaved Dde protecting group was measured at 290 nm in the washing solution after the first, 10^{th}, and 15^{th} incubation step.

Afterwards, the fluorescent dye FITC was coupled to the ε-amino group of the C-terminal lysine side chain. FITC (2 eq, 15.576 mg) was dissolved in 500 µl DMF before DIPEA (4 eq, 13.68 µl) was added. The solution was added to the resin and incubated overnight at room temperature and under light protection. After 24 hours of incubation the resin was washed thoroughly with DMF and DCM.

2.3.4 Peptide cleavage

A mixture of 95% TFA, 2.5% water, and 2.5% TIPS was used to detach the peptide from the resin. The cleaved peptide was precipitated using 40 ml of a precooled 1:1 mixture of MTBE and *N*-hexane. The resin was incubated with the cleavage cocktail for one hour at room temperature. Subsequently, the mixture was transferred into the precooled precipitation solution, shaken, and stored for ten minutes at 4 – 8 °C and ten more minutes at -20°C. After successful precipitation, centrifugation for 15 minutes, and decantation of the supernatant the peptide was dried at room temperature. At last, the precipitate was lyophilized with Freeze-Dryer Alpha 1-4 LDplus (Martin Christ Gefriertrocknungsanlagen GmbH, Osterode am Harz, Germany) and stored at 4 – 8 °C under light protection until further use.

2.4 Solubility testing

To find an adequate eluent for analysis and purification with RP-HPLC, the solubility of the synthesized peptides was determined in water, methanol, and an acetonitrile/water mixture. Concentrations of 0.1 mg/ml up to 1 mg/ml were tested. To accelerate the solubility process ultrasonication (20 min, 20 °C, 100% power) was performed with sonicator Bandelin Super 10P (BANDELIN electronic GmbH & Co. KG, Berlin, Germany).

2.5 Purification with preparative RP-HPLC

The crude product was purified using a Büchi Pure C-850 FlashPrep preparative reverse-phase high-performance liquid chromatography (HPLC) machine (Büchi Labortechnik GmbH, Wehingen, Germany) with a PrepPure C18-RP column (100 Å, 5 µm). The sample preparation was executed as follows: 5 ml of a solution with a concentration of 0.5 mg/ml of each peptide were prepared by dissolving in a mixture of 20% (V/V) acetonitrile in water. Subsequently, ultrasonication (20 min, 20 °C, 100% power), following centrifugation (10

minutes, 16 °C, 10.000 rpm), and filtration of the sample was performed. Samples of peptide$_{1-10}$, $_{45-55,}$ and all three control peptides were filtered with a CHROMAFIL Xtra PTFE-20/13 filter with a pore size of 0.2 µm. For peptide$_{132-142}$ a glass fiber filter with the pore size of 1 µm was used.

The mobile phase consisted of solvent A water acidified with 0.1% TFA and solvent B acetonitrile acidified with 0.08% TFA. To guarantee efficient separation different conditions were chosen. Samples of peptide$_{45-55}$ and $_{132-142}$, respectively, were separated with the following increasing concentration of solvent B: 0 to 20 minutes 10% to 60%, and 20 to 25 minutes from 60% to 100%. Samples of control peptide$_{45-55}$ and $_{132-142}$, and of peptide$_{1-10}$ were separated with the difference of starting with a linear gradient of 5 minutes of 5% acetonitrile, 5 to 20 minutes from 5% to 60% and 20 to 25 minutes 60% to 100%. A flow rate of 5 ml/min was selected, and the eluents were detected at 214 nm, 280 nm, and 440 nm. The peaks resulting from the purification process were collected separately and analyzed by analytical RP-HPLC. Because of the chosen eluent the final peptides were present as TFA salts by forming salts with basic side chains of arginine, lysine, and histidine.

2.6 Sample storage

The purified peptides were split into 300 µl to 600 µl aliquots. TFA and acetonitrile residues were removed by evaporation via vacuum concentrator centrifuge Univapo 150 H (UniEquip Laborgerätebau und Vertriebs GmbH, Freital, Germany). Subsequently, the samples were frozen at -80 °C, lyophilized with Freeze-Dryer Alpha 1-4 LDplus (Martin Christ Gefriertrocknungsanlagen GmbH, Osterode am Harz, Germany), and stored at 4-8 °C in tubes under light protection. Each tube contained approximately 0.1 to 0.4 mg peptide.

2.7 Analytics

2.7.1 Analytical RP-HPLC

The purity of the peptides before and after purification was analyzed via a Nexera XR analytical HPLC (Shimadzu Corp., Kyoto, Japan) using an analytical reverse-phase Nucleodur C18 column (Machery-Nagel GmbH & Co. KG, Düren, Germany) and a UV-diode array detector. A gradient elution protocol was chosen at a flow rate of 1 ml/min. After the injection of the 5 µl sample, the gradient started at 20% acetonitrile with 0.08% TFA and 80%

water with 0.1% TFA turning into 80% and 20%, respectively, within 15 minutes. After the completed run the purity was assessed at 440 nm using the software LabSolutions Shimadzu. After purification the fraction with the most prominent peak at 440 nm was determined.

2.7.2 Mass spectrometry

The identity of the peptides was confirmed by high-resolution mass spectrometry. For this purpose, a turbo ion source ESI X500 QTOF mass spectrometer (AB Sciex, Darmstadt, Germany) was used and kindly provided and executed by Dr. Ammar Tahir (University of Vienna, Austria). Specific settings were kept as follows: heater temperature at 500 °C, ion source gas 1 set to 30 psi, ion source gas 2 set to 30 psi, and curtain gas set to 45 psi. To achieve negative/positive ion mode ionization, spray voltages of -4,5 KV / +5,0 KV were applied. TOFMS scans were executed with an m/z range from 100 to 1900. To prepare samples, TFA residues were removed by spinning in a vacuum concentrator centrifuge Univapo 150 H (UniEquip, Freital, Germany) for 15 minutes without and 25 minutes with power, respectively.

2.8 Sample preparation

2.8.1 Peptide quantification

Determination of the peptide samples concentration was necessary for adequate and reproductive sample preparation for the cell assays. Measurement of absorbance at 280 nm allows the quantification of peptides by equation of the Beer's Law. This is due to aromatic residues in amino acid side chains which show high UV-absorbance properties. Specifically, tyrosine (Tyr, Y) and tryptophane (Trp, W) and to a lesser degree cysteine (Cys, C) absorb at 280 nm. Phenylalanine (Phe, F) also has an aromatic side chain but absorbs UV rays from 240 to 265 nm. (23, 24) For peptide quantification, firstly the establishment of the molar extinction coefficient of the unlabeled peptide is necessary. The molar extinction factor is related to the number of residues of the amino acids W, Y, and C. Its value is calculated by the weighted sum of the molar absorption coefficients at 280 nm of the amino acids as shown in the following equation: (23, 24)

$$\varepsilon = (nW \cdot 5500) + (nY \cdot 1490) + (nC \cdot 125)$$

$$n \ldots number\ of\ residues\ in\ a\ peptide$$

$$W \ldots tryptophane$$

$$Y \ldots tyrosine$$

$$C \ldots cysteine$$

$$\varepsilon \ldots molar\ extinction\ coefficient\ of\ peptide$$

The molar concentration of a peptide in a solution can be calculated from the degree of absorbance at 280 nm. FITC also absorbs light to a certain degree at 280 nm. The maximum absorption wavelength of FITC alone is 495 nm, respectively. To adjust for the absorbance at 280 nm by FITC a correction factor and the absorbance of the labeled peptide solution at 495 nm were included. The correction factor CF is obtained by division of absorbance of FITC at 280 nm and 495 nm and is listed in the Thermo Scientific Tech Tip #31 with the value of 0.3. The molar concentration was calculated using the following equation: (25)

$$Protein\ concentration\ M = \frac{A_{280} - (A_{max} \cdot CF)}{\varepsilon} \cdot DF$$

$$A_{280} \ldots absorbance\ of\ labeled\ peptide\ at\ 280\ nm$$

$$A_{max} \ldots absorbance\ of\ labeled\ peptide\ at\ 495\ nm$$

$$CF \ldots correction\ factor = 0.3$$

$$DF \ldots dilution\ factor$$

$$\varepsilon \ldots molar\ extinction\ coefficient\ of\ peptide$$

For the cell assays the purified and lyophilized peptides were dissolved in 200 µl 0.003 M PBS buffer containing Ca^{2+} and Mg^{2+} with pH 7.04 to obtain a peptide stock solution. Absorption at 280 and 495 nm was then measured on the Lambda XLS UV/VIS spectrometer (PerkinElmer Inc., Waltham, MA, USA) in micro UV-cuvettes. The samples had to be diluted so the measured absorption was between 0.2 and 1. The calculation of the molar concentration was executed using the previously described equation.

For cell binding assays a dilution series with eleven dilutions beginning from 50 µM and continuing with 40 µM, 30 µM, 25 µM, 20 µM, 15 µM, 10 µM, 7 µM, 5 µM, 3 µM, and 1 µM was prepared. For inhibition cell assays 50 µM peptide solutions were used.
All dilution steps were made with the previously mentioned PBS buffer. All samples were prepared on the experiment day and under light protection.

2.8.2 Fluorescence intensity

Prior to the experiments the fluorescence intensity of the samples was directly measured with a TECAN Infinite® M200 Pro microplate-reader (Tecan Group Ltd., Männedorf, Switzerland) (at 485/525 nm ex/em with 50% gain). This secured that the measured fluorescence signal was the same for every tested peptide. To additionally control the fluorescent intensity the degree of FITC labeling was assessed. In this context two parameters were calculated to evaluate the degree of FITC labeling: the A_{280}/A_{495} ratio and the f/p molar ratio. (25)

Firstly, the peptide solution was measured at 280 nm as well as at 495 nm. Afterwards, the ratio was calculated as follows:

$$ratio = \frac{A_{280}}{A_{495}}$$

$$A_{280} \dots absorbance\ of\ labeled\ peptide\ at\ 280\ nm$$

$$A_{max} \dots absorbance\ of\ labeled\ peptide\ at\ 495\ nm$$

Additionally, the f/p molar ratio was calculated which predicts the average moles of fluorescent dye per mole peptide. It was determined by the following equation, calculating the FITC and peptide molar concentrations separately and then obtaining the quotient: (25)

$$Moles\ dye\ per\ mole\ peptide = \frac{A_{max}\ of\ labeled\ peptide}{\varepsilon' \cdot peptide\ concentration\ (M)} \cdot DF$$

$$A_{max} \ldots absorbance\ of\ labeled\ peptide\ at\ 495\ nm$$

$$\varepsilon' \ldots molar\ extinction\ coefficient\ of\ FITC \ldots 68000\ M^{-1} \cdot cm^{-1}$$

$$M \ldots molar\ concentration\ of\ peptide$$

$$DF \ldots dilution\ factor$$

2.9 Cell culture

For cell experiments two bladder cell lines, 5637 and SV HUC-1 were utilized. The 5637 cell line is a human epithelial cancer cell line isolated from urinary bladder cancer with grade 2 carcinoma. The SV HUC-1 cell line is derived from non-cancerous uroepithelial human cells. Both cell lines were obtained from ATCC, Rockville, MD, USA. Cells were cultured in T75 cell culture flasks in a 37 °C, humidified 5% CO_2 / 95% air atmosphere.

5637 cells were cultivated in Roswell Park Memorial Institute (RPMI) medium supplemented with 10% fetal calf serum (FCS) and used between passages 68 to 81.

SV HUC-1 cells were grown in F12K medium and were utilized between passages 55 to 65. Sub-cultivation was carried out at about 80% confluency by treatment with 0.25% trypsin + 0.038% EDTA.

2.10 Binding studies

The binding properties of the peptides to the cell surface were examined using 5637 and SV HUC-1 single cells. The investigated peptides were peptide$_{45\text{-}55}$, peptide$_{132\text{-}142}$, and their corresponding control peptides$_{45\text{-}55}$ and $_{132\text{-}142}$, respectively. The experiment was set as follows and implemented likewise for both cell lines: cells were grown to approximately 80% confluency, then sub-cultivated with 0.25% trypsin + 0.038% EDTA, adjusted to a cell count of 3 x 10^6 cells per ml with medium and precooled. 50 µl of the cell suspension were then incubated with 10 µl of the peptide solution of interest. The peptides were tested in a concentration range from 1 µM, 3 µM, 5 µM, 7 µM, 10 µM, 15 µM, 20 µM, 25 µM, 30 µM, 40 µM to 50 µM. After the cells were incubated with the peptide solution for two hours at 37°C, the cells were transferred into 940 µl isotone HEPES pH 7.4. The cell-bound peptides were

assessed using Gallios™ Flow Cytometer (Beckman Coulter Inc., Indianapolis, IN, USA) at 488/525 nm ex/em.

2.11 Inhibition studies

To evaluate the binding specificity of the peptides, single-cell inhibition studies with both 5637 and SV HUC-1 cells were performed. The investigated peptides were $peptide_{45\text{-}55}$, $peptide_{132\text{-}142,}$ and their corresponding control $peptides_{45\text{-}55}$ and $_{132\text{-}142}$, respectively.

To investigate if the cell adhesion of the peptides was mediated by binding to mannose receptors, α-D-mannose was used as an inhibiting agent. As a negative control α-D-galactose solutions were utilized. (26)

After subcultivation, the cell suspension was adjusted to 3,75 x 10^6 cells per ml with medium and precooled. Then 10 µl of the 50 µM peptide solution were incubated with 10 µl of α–D-mannose or α–D-galactose solution, respectively, for 30 minutes at 37 °C. The monosaccharide solutions ranged from molarities of 5 mM, 1 mM, 0,5 mM, 0,1 mM, 50 µM, 10 µM to 1 µM and were prepared in PBS buffer with Ca^{2+} and Mg^{2+}. Afterwards, 40 µl of the cell suspension of interest were added and incubated for two additional hours at 37 °C. After completed incubation the sample was transmitted to 940 µl isotone HEPES pH 7.4. Inhibition of cell interaction between peptide and single cells was evaluated at 488/525 nm (ex/em) using Gallios™ Flow Cytometer (Beckman Coulter Inc., Indianapolis, IN, USA).

2.12 Fluorescence microscopic analysis

For visualization of cell binding properties and possible internalization of the peptides fluorescence, microscopic analysis was performed with 5637 cell monolayers. The investigated peptides were $peptide_{45\text{-}55}$, $peptide_{132\text{-}142,}$ and their corresponding control $peptides_{45\text{-}55}$ and $_{132\text{-}142}$, respectively.

Prior to cell culture, flexiPERM® silicone inserts, object slides, and Petri dishes were treated with 70% (V/V) ethanol and allowed to dry under a laminar flow hood. Cells were seeded at a density of 10 x 10^3 cells/160 µl on microscope slides mounted with flexiPERM® and grown for four days.

The cells were washed once with 100 µl isotone HEPES pH 7.4. Then 50 µl of 50 µM peptide solution were added to the cell layer with additional 2 µl aqueous HOECHST 33342 solution (1 mg/ml) to stain the nucleus of the cells and incubated for 30 minutes at 37 °C.

After incubation the sample was discarded with a pipette, and the cell layer was washed twice with 100 µl isotone HEPES pH 7.4 before adding 50 µl of HEPES.

To preserve the state of the cells and avoid fluorescent dyes from entering the cells, the cells were fixed with 50 µl 4% (m/V) paraformaldehyde solution and incubated for 15 minutes. Afterwards, 100 µl of 100 mM ammonium chloride solution were transferred into the well to quench the cells, and incubation was continued for further 15 minutes. Afterwards, the ammonium chloride was removed and replaced with 52 µl of HEPES.

As a last step, 5 µl of ALEXA-WGA solution (0.1 mg/ml) were added to stain the cell membrane, incubated for 15 minutes, and afterwards washed two times with 100 µl HEPES. Lastly, the cell layer was treated with 50 µl isotone HEPES pH 7.4 before cell imaging with the Zeiss Epifluorescence Axio Observer fluorescent microscope (Carl Zeiss Microscopy GmbH, Oberkochen, Germany).

2.13 Statistical analysis

GraphPad Prism software (version 10) was used for graphics and statistical analysis as described in the figure legends. The groups were compared to each other using a two-way ANOVA to calculate the *p* values. Differences were considered as statically significant at $p < 0.05$. All data were presented as mean ± standard deviation.

3 Results and Discussion

3.1 Characterization of the synthesized peptides

3.1.1 Peptide$_{1-10}$

Peptide$_{1-10}$ is arranged in the primary sequence FACKTANGTAK with Phe1 positioned on the amino terminus, continuing up to Ala10 and ending with lysine at the carboxyl terminus. Peptide$_{1-10}$ comprises the ten first amino acid residues of FimH and contains the amino acid Phe1 which was shown to be crucial for carbohydrate binding properties. (18) Phe1 is part of the carbohydrate-binding pocket in the bacterial lectin FimH and interacts with the α-D-mannose molecule via hydrophobic interactions. (14, 18)

Likewise, the corresponding control peptide$_{1-10}$ consists of the same first ten amino acids as the peptide$_{1-10}$, however in the random order ATACNKGTFAK.

The following two Figures 4 and 5 give an overview of the chemical formulas and structures of peptide$_{1-10}$ and its associated control peptide$_{1-10}$.

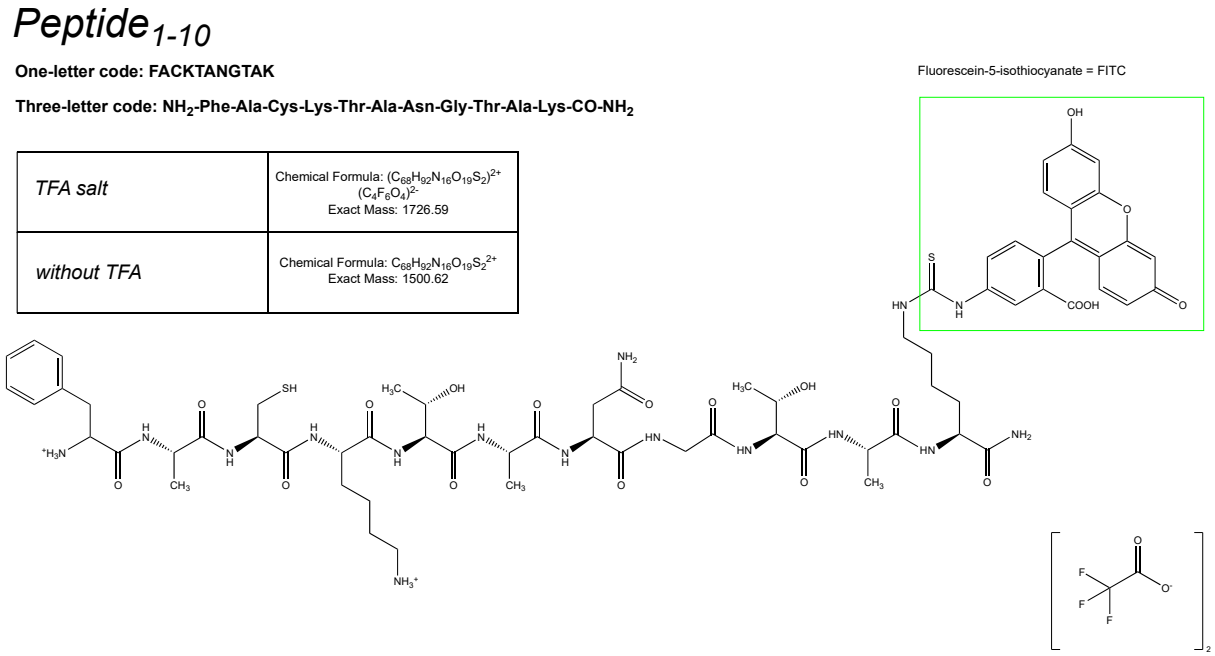

Figure 4: Molecular characterization of peptide $_{1-10}$ (created with ChemDraw)

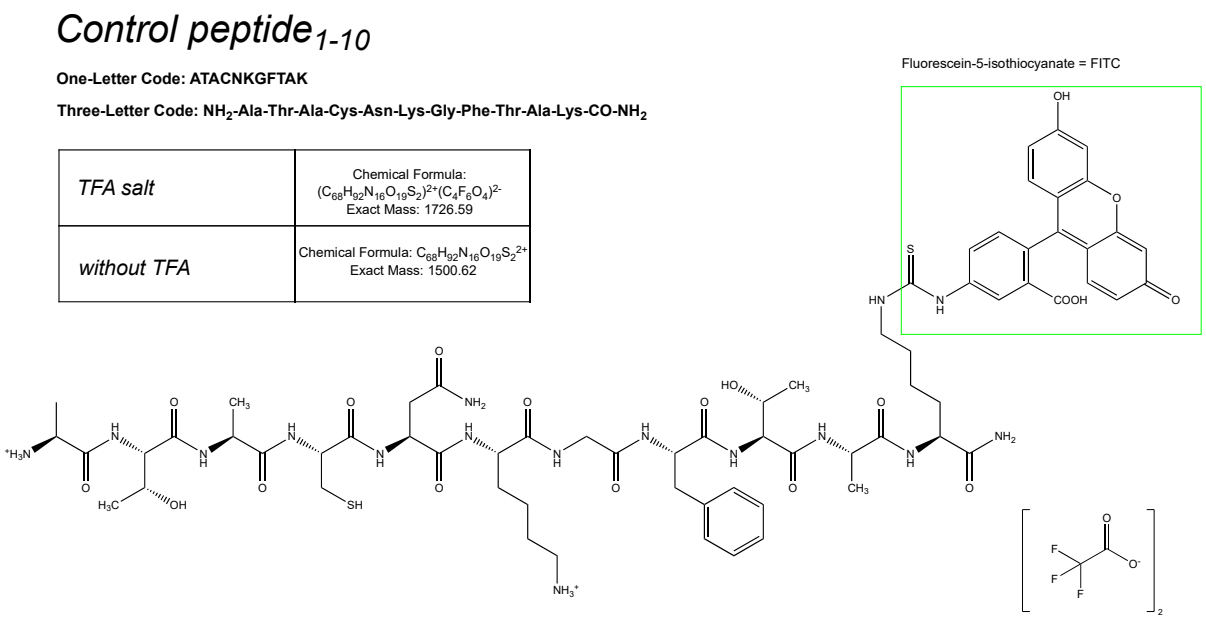

Figure 5: Molecular characterization of control peptide$_{1\text{-}10}$ (created with ChemDraw)

3.1.2 Peptide$_{45\text{-}55}$

Peptide$_{45\text{-}55}$ consists of the eleven amino acids 45 to 55 of FimH with the five amino acids Asn46, Asp47, Tyr48, Ile52, and Asp54 which were found to be detrimental in the binding of the FimH lectin domain to α-D-mannose. (14, 18) With the primary sequence of HNDYPETITDYK His45 marks the initial amino acid positioned at the N-terminus, extending through Tyr55, and concluding with lysine at the C-terminus. Asn46, Asp47, Tyr48, Ile52, and Asp54 are part of the lining of the carbohydrate pocket of FimH and are especially crucial for the carbohydrate-binding properties of FimH. The amino acids Asn46, Asp47, and Asp54 connect with α-D-mannose in the binding pocket via hydrogen bonds. Furthermore, Tyr48 and Ile52 are part of the hydrophobic ridge surrounding the binding pocket to increase the affinity to α-D-mannose. (14, 18)

The control peptide$_{45\text{-}55}$ contains the identical amino acids but in the random order PEDTYHNDTIYK. The chemical formulas and the structures of both the investigated peptide and its control peptide are displayed in Figures 6 and 7.

Peptide$_{45\text{-}55}$

One-Letter Code: HNDYPETITDYK

Three-Letter Code: NH_2-His-Asn-Asp-Tyr-Pro-Glu-Thr-Ile-Thr-Asp-Tyr-Lys-CO-NH_2

TFA salt	Chemical Formula: $(C_{87}H_{108}N_{18}O_{28}S)^{2+}$ $(C_2F_3O_2)_2^{2-}$ Exact Mass: 2110.7
without TFA	Chemical Formula: $C_{87}H_{108}N_{18}O_{28}S^{2+}$ Exact Mass: 1884.73

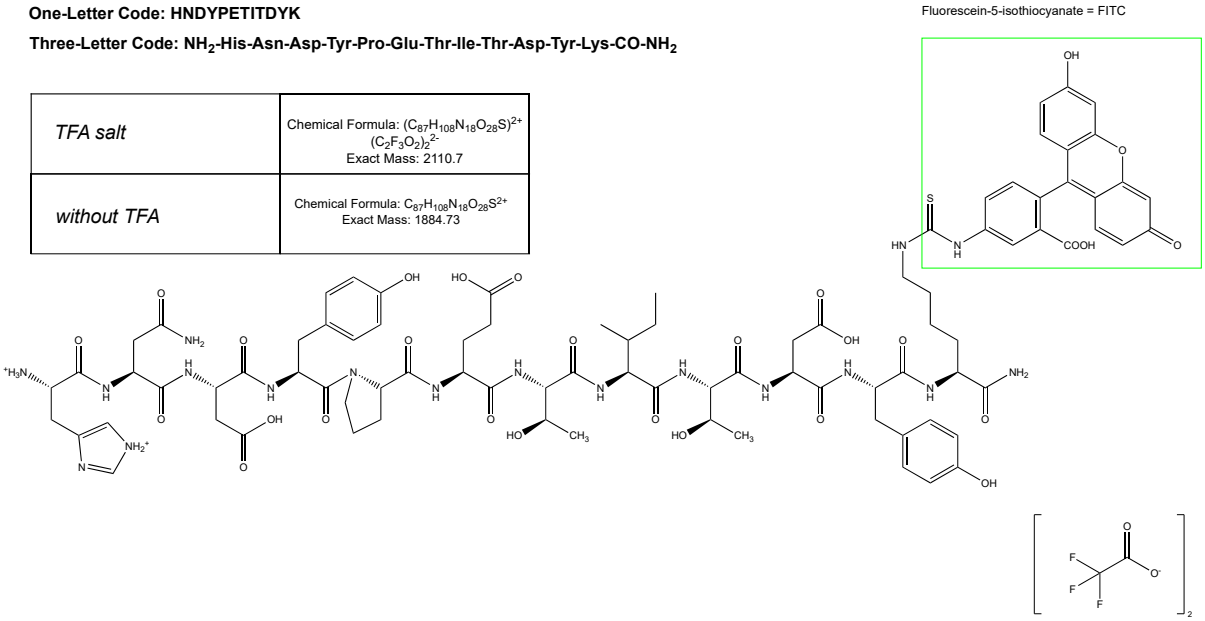

Figure 6: Molecular characterization of peptide$_{45\text{-}55}$ (created with ChemDraw)

Control peptide$_{45\text{-}55}$

One-Letter Code: PEDTYHNDTIYK

Three-Letter Code: NH_2-Pro-Glu-Asp-Thr-Tyr-His-Asn-Asp-Thr-Ile-Tyr-Lys-CO-NH_2

TFA salt	Chemical Formula: $(C_{87}H_{107}N_{18}O_{28}S)^{+}$ $(C_2F_3O_2)^{-}$ Exact Mass: 1996.71
without TFA	Chemical Formula: $C_{87}H_{107}N_{18}O_{28}S^{+}$ Exact Mass: 1883.72

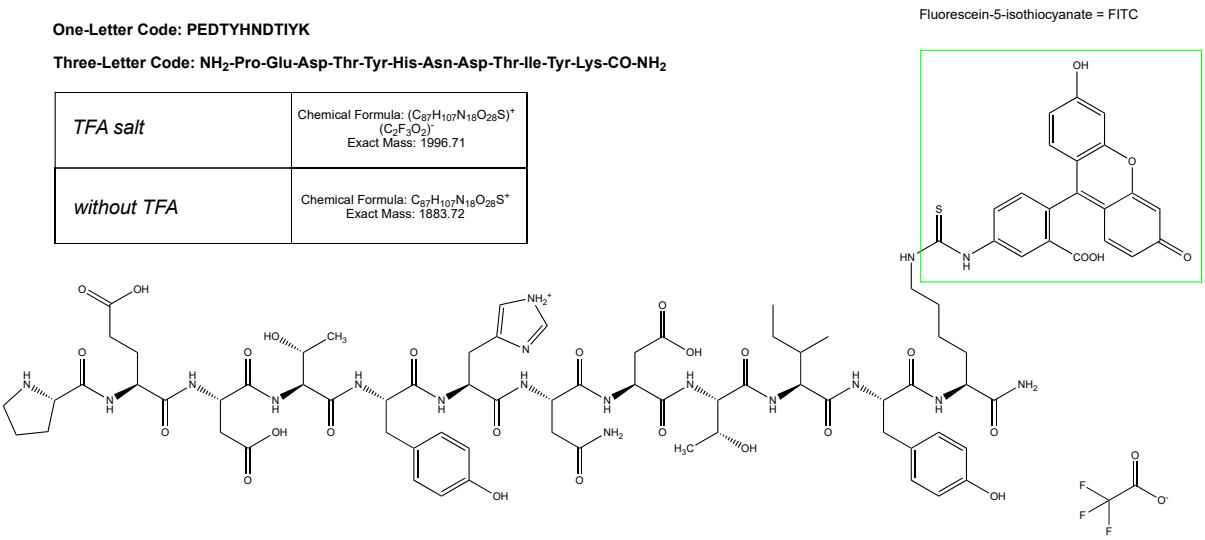

Figure 7: Molecular characterization of control peptide$_{45\text{-}55}$ (created with ChemDraw)

3.1.3 Peptide$_{132\text{-}142}$

Peptide$_{132\text{-}142}$ comprises the eleven amino acids 132 to 142 of FimH, containing the six amino acids Gln133, Asn135, Tyr137, Asn138, Asp140, and Asp141 which directly interact with α-D-mannose. (14, 18) With the primary sequence RQTNNYNSDDFK the initial amino acid is Arg132, continuing to Phe142 and terminating with an additional lysine at the C-terminus. Gln133, Asn135, Tyr137, Asn138, Asp140, and Asp141 are part of the carbohydrate-binding site. (14) Gln133, Asn135, Asp140, and Phe142 interact with the single α-D-mannose molecule via hydrogen bonds and hydrophobic forces. Moreover, Gln133 is responsible for stabilizing the binding pocket. Additionally, Phe142 is part of the affinity-enhancing hydrophobic ridge in the binding pocket. (18)

Likewise, the control peptide$_{132\text{-}142}$ consists of the identical eleven amino acids but in a random order FRDTQNSYNDNK. Chemical formulas and structures of the corresponding peptides are displayed in Figures 8 and 9.

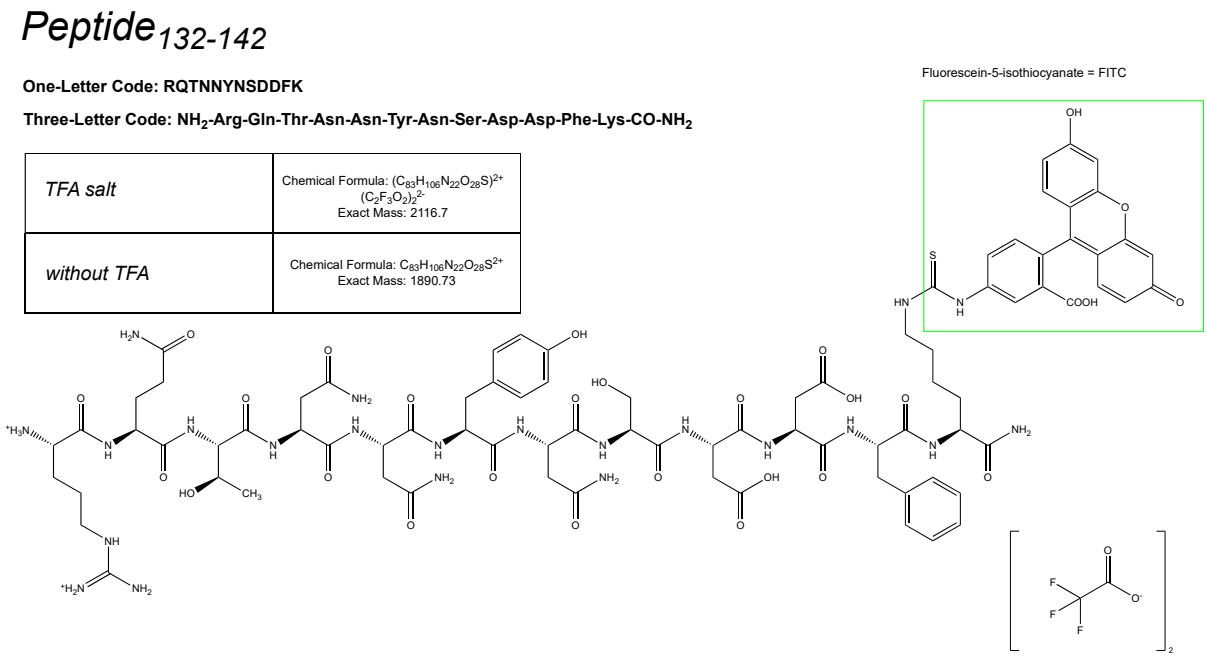

Figure 8: Molecular characterization of peptide$_{132\text{-}142}$ (created with ChemDraw)

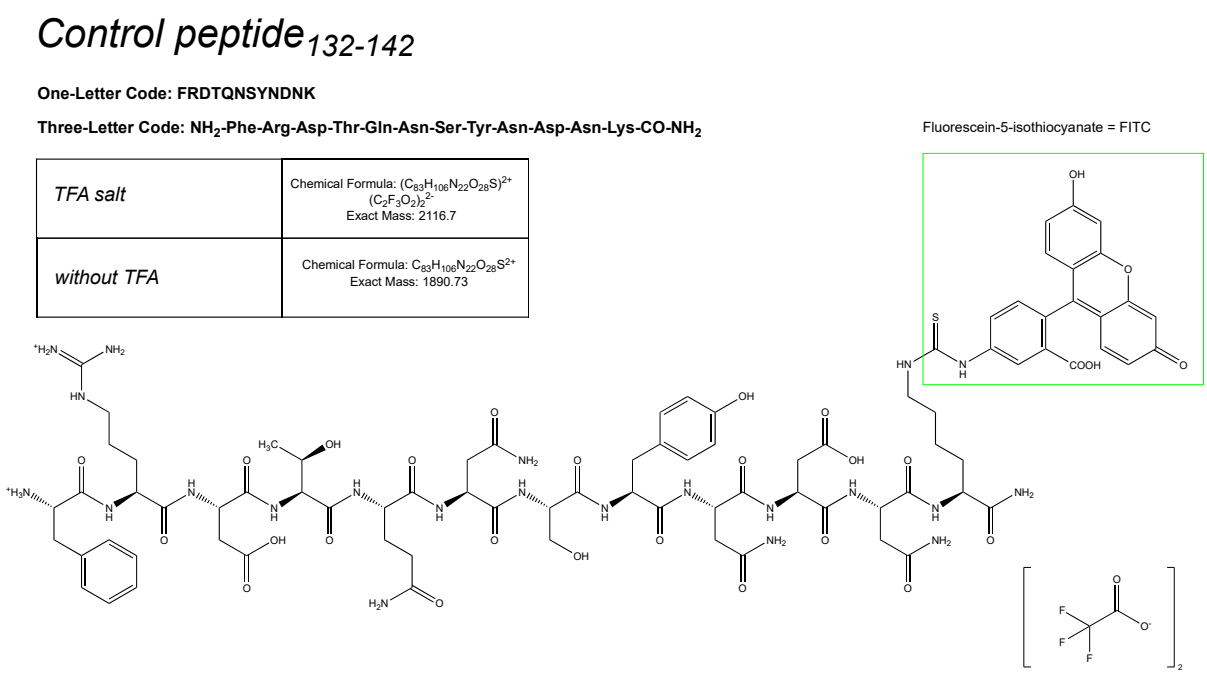

Figure 9: Molecular characterization of control peptide$_{132-142}$ (created with ChemDraw)

3.2 Solubility

The solubility of the peptides$_{1-10}$, $_{45-55,}$ and $_{132-142}$, respectively, was tested with different solvents. Before purification the aim was to find the adequate eluent for both preparative and analytical RP-HPLC. An overview of the solubility is given in Table 1.

Table 1: solubility of peptides$_{1-10}$, $_{45-55,}$ and $_{132-142}$.

	water	*MeOH*	*20% ACN in water*	*PBS buffer pH 7.4*
peptide$_{1-10}$	✓	✗	✓	✓
peptide$_{45-55}$	✓	✗	✓	✓
peptide$_{132-142}$	✗	✓	✓	✓

Peptide$_{1-10}$ and peptide$_{45-55}$ were easily soluble in water, compared to peptide$_{132-142}$ which was insoluble. Interestingly, methanol could be identified as the only solvent that was able to solve peptide$_{132-142}$ while peptide$_{1-10}$ and $_{45-55}$, respectively, were insoluble.

All peptides including their corresponding control peptides were soluble in a mixture of 20% (V/V) acetonitrile in water and in PBS buffer with Ca^{2+} and Mg^{2+} pH 7.04. Therefore,

acetonitrile in water was used as an eluent in HPLC, whereas the PBS buffer was chosen as a cell assay medium.

3.3 Peptide Purification

After successful synthesis all peptides were purified with preparative RP-HPLC, and their purity was confirmed via analytical RP-HPLC. While control peptide$_{1\text{-}10}$ was successfully purified, definitive purification was not achieved for peptide$_{1\text{-}10}$ as post-purification RP-HPLC analysis showed two distinctive peaks at retention times of 4.893 and 5.345 minutes, respectively. This suggests an incomplete purification due to the presence of peptide fragments that could not be removed by preparative RP-HPLC (see Appendix 3 for analytical RP-HPLC spectra).

Purification of the remaining peptides$_{45\text{-}55}$ and $_{132\text{-}142}$ and their corresponding control peptides was successfully achieved (see Appendix 3 for analytical RP-HPLC spectra).

3.4 Mass spectrometry

3.4.1 MS of peptide$_{1\text{-}10}$

The identity and structure of the peptide$_{1\text{-}10}$ and its control peptide$_{1\text{-}10}$ were successfully confirmed by mass spectrometry (see Appendix 4 for mass spectrums).

Peptide$_{1\text{-}10}$

[M+H] calcd for $C_{68}H_{91}N_{16}O_{19}S_2^+$ 1499.62, found at 1499.39 (m/z).

[M+2H] calcd for 750.31 (1499.62/2), found at 750.28.

[M+3H] calcd for 500.54 (1499.62/2), found at 500.82.

Control peptide$_{1\text{-}10}$

[M+H] calcd for $C_{68}H_{91}N_{16}O_{19}S_2^+$ 1499.62, found at 1499.6006 (m/z).

[M+2H] calcd for 750.31, found at 750.3024.

[M+3H] calcd for 500.54, found at 500,8709.

3.4.2 MS of peptide$_{45-55}$

The structure and identity of peptide$_{45-55}$ and its corresponding control peptide$_{45-55}$ were confirmed by mass spectrometry (see Appendix 4 for mass spectra).

Peptide$_{45-55}$

[M+H] calcd for $C_{87}H_{107}N_{18}O_{28}S^+$ 1883.73, found at 1884.42 (m/z).

[M+2H] calcd for 942.365 (1884.73/2), found at 942.52.

[M+3H] calcd for 628.58 (1885.73/3), found at 628.74.

Control peptide$_{45-55}$

[M+H] calcd for $C_{87}H_{107}N_{18}O_{28}S^+$ 1883.72, found at 1884.7101 (m/z).

[M+2H] calcd for 942.36 (1884.72/2), found at 942.36.

[M+3H] calcd for 628.57 (1885.72/3), found at 628.5739.

3.4.3 MS of peptide$_{132-142}$

The structure and identity of peptide$_{132-142}$ and its corresponding control peptide$_{132-142}$ were successfully confirmed by mass spectrometry (see Appendix 4 for mass spectrums).

Peptide$_{132-142}$

[M+H] calcd for $C_{83}H_{105}N_{22}O_{28}S^+$ 1889.73, found at 1890.35 (m/z).

[M+2H] calcd for 945.365 (1890.73/2), found at 945.49.

[M+3H] calcd for 630.58 (1891.73/3), found at 630.68.

Control peptide$_{132-142}$

[M+H] calcd for $C_{83}H_{105}N_{22}O_{28}S^+$ 1889.73, found at 1890.7152 (m/z).

[M+2H] calcd for 945.365 (1890.73/2), found at 945.3575.

[M+3H] calcd for 630.58 (1891.73/3), found at 630.9077.

3.5 Sample preparation

3.5.1 Determination of the molar extinction factor

For photometric quantification of the peptides, the molar extinction factors of the peptides were obtained at 280 nm. The molar extinction factors ε of the final peptides were calculated by summing the molar extinction factors of tyrosine, tryptophane, and cysteine (see 2.8.1 "Peptide quantification" for the molar extinction factor equation).

For $peptide_{45\text{-}55}$ and control $peptide_{45\text{-}55}$ a molar extinction factor ε of 2980 $M^{-1}.cm^{-1}$ was calculated, with two tyrosine residues in each primary sequence.

For $peptide_{132\text{-}142}$ and control $peptide_{132\text{-}142}$ a molar extinction factor ε of 1490 $M^{-1}.cm^{-1}$ was determined, with one tyrosine residue in each primary sequence.

For $peptide_{1\text{-}10}$ and its control $peptide_{1\text{-}10}$ no molar extinction factor ε was calculated. The measurement of the peptide concentration at 280 nm requires the presence of the amino acids tryptophane, tyrosine, and to a lesser extent cysteine. $Peptide_{1\text{-}10}$ and the control $peptide_{1\text{-}10}$, respectively, do not contain any tyrosine or tryptophane residue in their sequence and only one cysteine residue. Cysteine on its own has a molar extinction factor of 125 (cf. tyrosine 1490 and tryptophane 5500) which does not allow sufficient quantification at 280 nm. Therefore, no further experiments and cell assays were performed with the $peptide_{1\text{-}10}$ and control $peptide_{1\text{-}10}$.

3.5.2 Measurement of the fluorescence intensity

Prior to the cell assays the fluorescence signals of the investigated peptide solutions were measured. Table 2 presents an overview of the mean fluorescence intensity with their standard deviation of solutions of peptide$_{45\text{-}55}$, peptide$_{132\text{-}142,}$ and their control peptides of the same molar concentration.

Table 2: mean fluorescence signal of peptide solutions. The data show the mean ± standard deviation.

	mean fluorescence signal ± SD	*n*
1 µM	233.50 ± 73.181	6
3 µM	1664.17 ± 301.758	6
5 µM	3539.00 ± 1135.762	6
7 µM	4823.25 ± 669.225	4
15 µM	13242.71 ± 1971.578	7
20 µM	15653.71 ± 1570.987	7
50 µM	28833.85 ± 2004.305	13

The data in Table 2 reveal that peptides of the same molar concentration showed similar intensity of fluorescence. This secured the comparison between different peptides during cell assays.

3.5.3 Determination of the A_{280}/A_{495} ratio

To assess the degree of FITC labeling the A_{28o}/A_{495} ratio was determined for every peptide sample. The peptide samples were dissolved in PBS buffer and measured at 280 nm and 495 nm. Afterwards, the quotient of the obtained absorptions was calculated. Table 3 below illustrates the mean A_{280}/A_{495} ratios of the peptides with their standard deviation. The calculations revealed that the ratios were similar between all the investigated peptides. This result suggests that the fluorescence signal remains consistent in all examined peptides which allowed the comparison between the different cell assays.

Table 3: A_{280}/A_{495} ratio of the peptides. The data show the mean ± standard deviation of n=5 experiments.

	mean A_{280}/A_{495} ratio ± SD
$peptide_{45-55}$	0.36 ± 0.016
control $peptide_{45-55}$	0.37 ± 0.006
$peptide_{132-142}$	0.34 ± 0.009
control $peptide_{132-142}$	0.34 ± 0.066

3.5.4 Determination of the f/p ratio

To further evaluate the FITC labeling degree, the f/p molar ratio was calculated. The f/p ratios of the peptides were then compared to each other. Table 4 provides the mean f/p ratios with their corresponding standard deviations of the same peptide from different experiments.

Table 4: f/p ratios of the peptides. The data show the mean f/p ratios ± standard deviation.

	mean f/p ratio ± SD	*n*
$peptide_{45-55}$	0.74 ± 0.148	5
control $peptide_{45-55}$	0.66 ± 0.056	5
$peptide_{132-142}$	0.58 ± 0.152	4
control $peptide_{132-142}$	0.63 ± 0.105	4

The calculated f/p molar ratios were not completely consistent. It can be observed from the data of Table 4 that $peptide_{45-55}$ had the highest mean f/p ratio, whereas $peptide_{132-142}$ had the lowest. A reason that can lead to different molar ratios of FITC labeling can be the insufficient coupling of FITC to the lysine side chain. Furthermore, despite peptide purification, unbound FITC due to potential de-coupling of FITC during storage could have led to different f/p molar ratios. In this case, dialysis of samples could be an option to ensure complete removal of unbound FITC. (25)

3.6 Binding studies

3.6.1 Peptide$_{45-55}$ vs control peptide$_{45-55}$

To investigate the cell surface binding properties of peptide$_{45-55}$ in comparison to its control peptide$_{45-55}$ single bladder cancer cells, and healthy human bladder cells, respectively, were used. Briefly, single cells were incubated with peptide solutions ranging from 1 µM to 50 µM at 37 °C for two hours. Afterwards, the cell-bound peptides were measured using flow cytometry at 488/525 ex/em (see 2.10 “Binding studies”). The measured fluorescence intensity directly correlated with the quantity of peptides bound to the cell surface.

The primary aim of using bladder cells was to evaluate the binding properties of the synthesized peptide$_{45-55}$ and its control peptide as FimH enables E. coli to efficiently adhere to and invade urinary bladder cells.

In figure 10 the mean measured fluorescence intensities of different concentrations of peptide$_{45-55}$ compared to its corresponding control peptide$_{45-55}$ on 5637 and SV HUC-1 single cells are shown.

On 5637 single cells peptide$_{45-55}$ consistently showed a higher fluorescence intensity at all concentrations compared to the control peptide$_{45-55.}$ The 50 µM sample of peptide$_{45-55}$ showed the highest cell surface affinity with a mean fluorescence intensity of 3.83 ± 0.107. Moreover, the binding affinity was increased by 32% compared to the control group at 50 µM. Surprisingly, the 20 µM sample of peptide$_{45-55}$ was found to show a higher fluorescence intensity than the 25 µM sample which however was due to a pipetting mistake (see Figure 10a). Furthermore, a two-way ANOVA revealed that the mean differences between the peptide and control group in samples of 10, 15, 20, 25, 40, and 50 µM were statistically significant (****, p-value <0.0001).

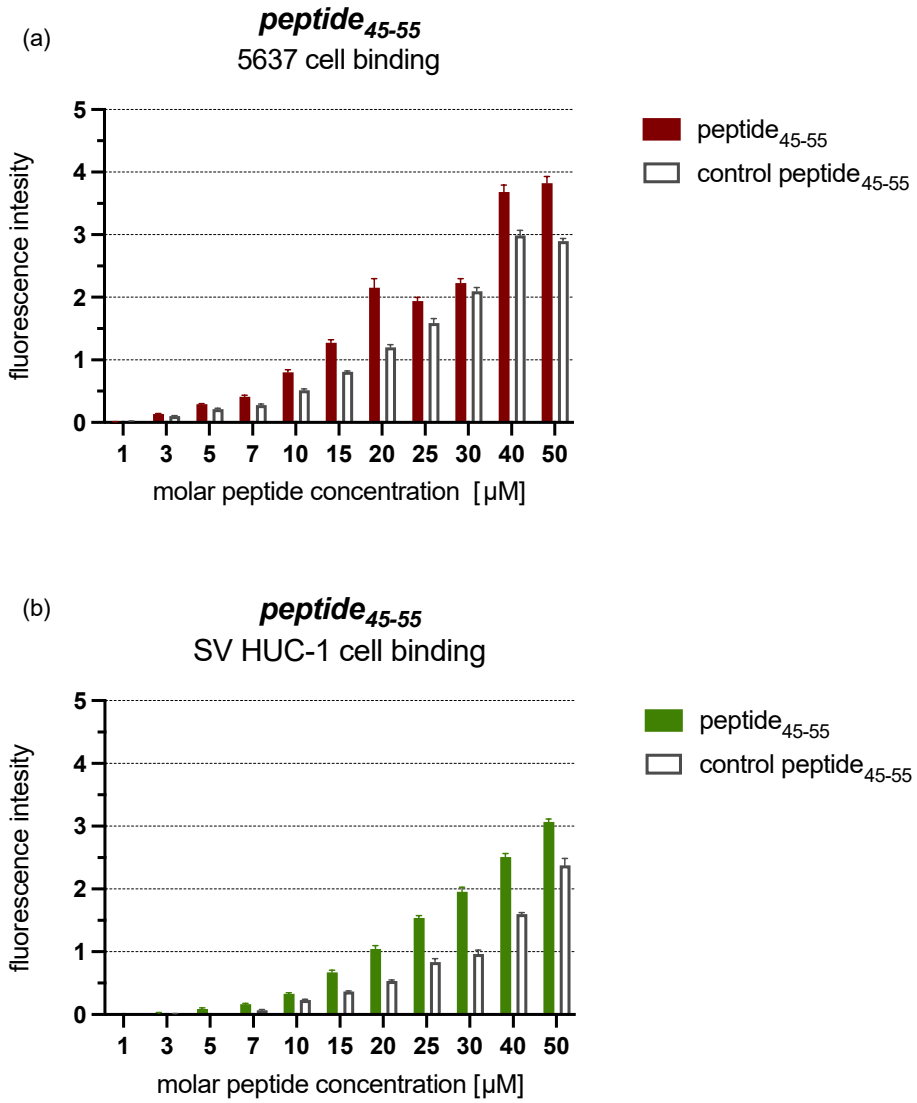

Figure 10: binding properties of peptide$_{45-55}$ compared to control peptide$_{45-55}$ ranging from 1 µM to 50 µM

The measured fluorescence intensity correlates with the cell binding properties of the peptides. (a) mean fluorescence intensity of peptide$_{45-55}$ in comparison to control peptide$_{45-55}$ on 5637 bladder cancer single cells. (b) mean fluorescence intensity of peptide$_{45-55}$ in comparison to control peptide$_{45-55}$ on SV HUC-1 bladder single cells. The data show the mean ± standard deviation of n=3 experiments. All graphs were created with GraphPad Prism.

To SV HUC-1 single cells peptide$_{45-55}$ also exhibited a higher binding affinity compared to the control peptide$_{45-55}$. The highest fluorescence intensity was observed at 50 µM with a fluorescence intensity of 3.07 ± 0.047 with an increase of the fluorescence signal compared to the control group by 29% (see Figure 10b). A two-way ANOVA showed that mean

differences at 15, 20, 25, 30, 40 µM, 50 µM (****, p-value <0.0001) and 10 µM (*, p-value 0.0434) between investigated peptide$_{45-55}$ and the control group were statistically significant.

Overall, peptide$_{45-55}$ showed a higher affinity to cell surfaces than the control peptide$_{45-55}$ in all concentrations and both cell lines. Peptide$_{45-55}$ has the same primary sequence as the FimH binding pocket from the residues 45 to 55, whereas the control peptide$_{45-55}$ consists of a random amino acid order. Therefore, a differently arranged primary sequence might result in a decrease in cell surface affinity. These results may suggest that the primary sequence of the peptide$_{45-55}$ identical to FimH enhances the binding properties to bladder cells.
Furthermore, the increase of fluorescence intensity between control and investigated peptide by 32% in 5637 cells and by 29% in SV HUC-1 cells, respectively, could indicate that an adequate primary sequence of peptide$_{45-55}$ has a higher influence on the binding to 5637 cells than to SV HUC-1 cells at 50 µM.

3.6.2 Peptide$_{132-142}$ vs control peptide$_{132-142}$

To examine the cell binding of peptide$_{132-142}$ compared to the control peptide$_{132-142}$ single bladder cancer cells and human healthy bladder cells were utilized. Single cells were incubated with peptide solutions ranging from 1 µM to 50 µM at 37 °C for two hours. Afterwards, the cell-bound peptides were measured using flow cytometry at 488/525 ex/em. The measured fluorescence intensity directly correlated with the binding properties of the peptides (see 2.10 “Binding studies”).
The main objective of using bladder cells was to investigate the binding properties of peptide$_{132-142}$ and its corresponding control peptide$_{132-142}$ as FimH enables E. coli to efficiently adhere to the human urinary bladder.
The measured fluorescence intensities of peptide$_{132-142}$ compared to control peptide$_{132-142}$ in increasing concentrations on 5637 and SV HUC-1 single cells, respectively, are set out in Figure 11.

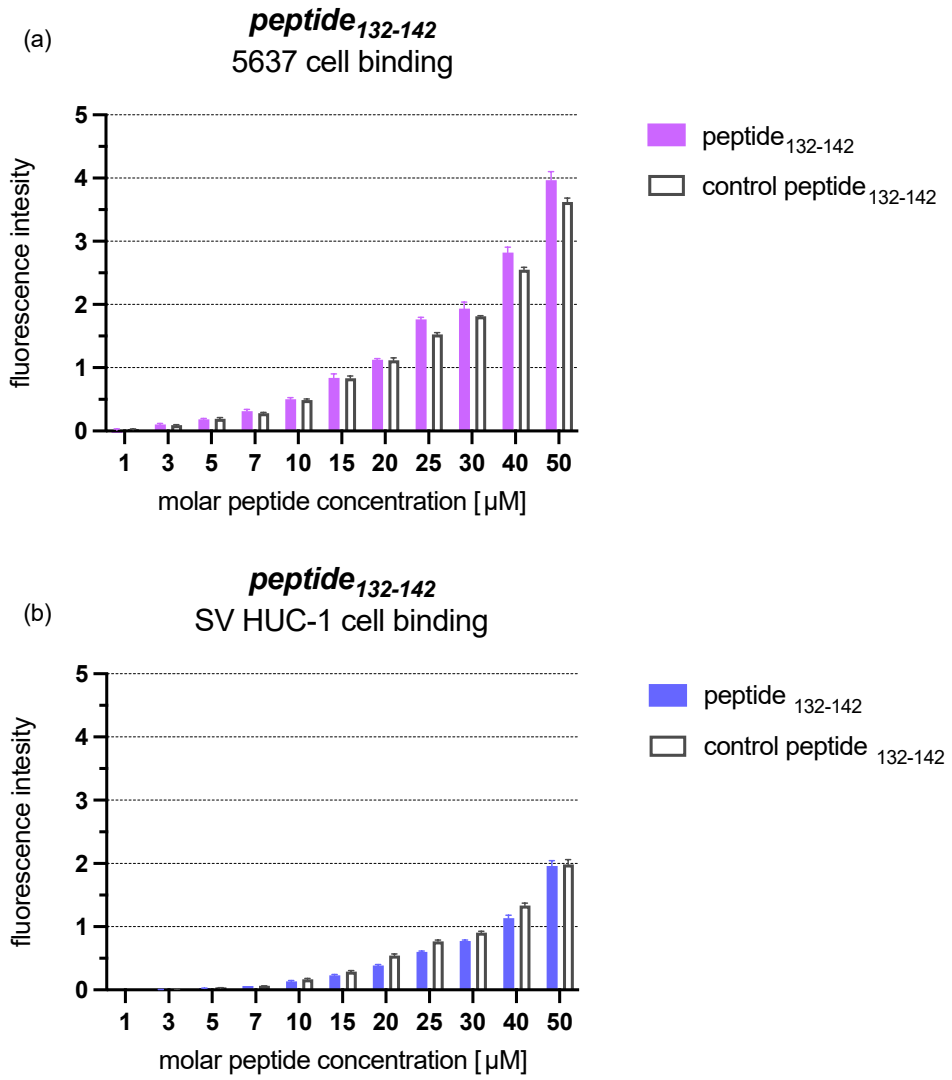

Figure 11: binding properties of peptide$_{132-142}$ compared to control peptide$_{132-142}$ ranging from 1 µM to 50 µM

The measured fluorescence intensity correlates with the binding properties of the peptides. (a) mean fluorescence intensity of peptide$_{132-142}$ in comparison to control peptide$_{132-142}$ on 5637 bladder cancer single cells. (b) mean fluorescence intensity of peptide$_{132-142}$ in comparison to control peptide$_{132-142}$ on SV HUC-1 single bladder cells. The data show the mean ± standard deviation of n=3 experiments. All graphs were created with GraphPad Prism.

On 5637 single cells peptide$_{132-142}$ showed a higher fluorescence intensity at all concentrations as compared to the control peptide$_{132-142}$. As expected, peptide$_{132-142}$ at 50 µM showed the highest fluorescence intensity of 3.97 ± 0.136 with an increase of 9% compared to the control peptide$_{132-142}$. The mean difference between the peptide and the control group at 25, 40, 50 µM (****, p-value < 0.0001), and 30 µM (*, p-value 0.0494) was statistically significant according to the executed two-way ANOVA (see figure 11a).

On SV HUC-1 single cells the control peptide$_{132\text{-}142}$ showed a higher fluorescence intensity compared to the peptide$_{132\text{-}142}$ from the molar concentrations of 3 to 50 µM and no difference at 1 µM. The highest fluorescence activity was measured at 50 µM for control peptide$_{132\text{-}142}$ at 1.98 ± 0.076, with an increase of 1.2% compared to peptide$_{132\text{-}142}$. Generally, the mean difference between the investigated peptide and the control peptide on SV HUC-1 cells was minimal, ranging from 0 to 0.20. A two-way ANOVA showed that the mean difference between peptide$_{132\text{-}142}$ and the control peptide$_{132\text{-}142}$ was statistically significant at 20, 25, 30, and 40 µM (****, p-value < 0.0001) (see figure 11b).

Taken together, these results indicate that peptide$_{132\text{-}142}$ showed a slightly higher affinity to 5637 single cells compared to the control peptide$_{132\text{-}142}$. However, on SV HUC-1 cells the control peptide$_{132\text{-}142}$ showed slightly higher binding properties and in some cases the same binding compared to the peptide$_{132\text{-}142}$. Moreover, the increase of fluorescence intensity in peptide$_{132\text{-}142}$ by 9% in 5637 cells compared to the control group, is lower than in peptide$_{45\text{-}55}$ in both cell lines (e.g., 32% and 29%, see 3.6.1 “peptide$_{45\text{-}55}$ vs control peptide$_{45\text{-}55}$”). These results may indicate that the primary sequence of peptide$_{132\text{-}142}$ which is identical to the FimH binding pocket from the residues 132 to 142, has a minor influence on the binding to the cell surface as compared to peptide$_{45\text{-}55}$.

3.6.3 Binding affinity on 5637 vs SV HUC-1

To further examine whether the peptides exhibited a higher binding affinity to cancerous or healthy bladder cells, the mean measured fluorescence intensities on 5637 single cells and SV HUC-1 single cells, respectively, were directly compared to each other and analyzed.
Figures 12 and 13 show a direct comparison of the measured fluorescence intensities of peptide$_{45\text{-}55}$ and peptide$_{132\text{-}142}$, respectively, at different concentrations on both 5637 and SV HUC-1 single cells.

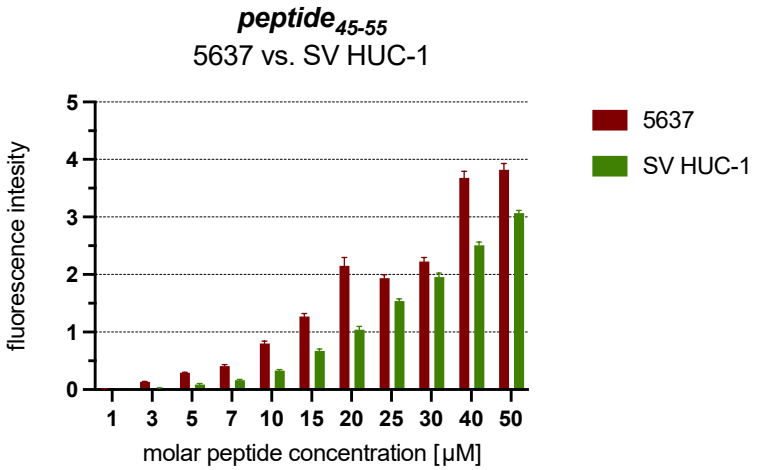

Figure 12: Comparison of cell surface affinity of peptide$_{45-55}$ from 1 µM to 50 µM on 5637 and SV HUC-1 single cells

The fluorescence intensity signal directly correlates with the cytoadhesive properties. Peptide$_{45-55}$ showed a higher fluorescence intensity on 5637 single cells at all molar concentrations as compared to SV HUC-1 cells. The data show the mean ± standard deviation of n=3 experiments. All graphs were created with GraphPad Prism.

All tested concentrations of peptide$_{45-55}$ showed a higher fluorescence intensity on 5637 single cells as compared to SV HUC-1 single cells. The affinity to 5637 cells at 50 µM is 25% higher compared to SV HUC-1 single cells (3.83 ± 0.107 compared to 3.07 ± 0.047). Therefore, peptide$_{45-55}$ exhibits higher cell associative properties to cancerous bladder cells than to healthy bladder cells (see Figure 12).

As can be seen from the graph in Figure 13, at all tested concentrations peptide$_{132-142}$ showed a higher cell-bound fluorescence to 5637 single cells compared to SV HUC-1 cells. Additionally, the mean measured fluorescence intensity of peptide$_{132-142}$ on 5637 single cells was 102% higher compared to SV HUC-1 single cells at 50 µM. These results indicate that peptide$_{132-142}$ also has a higher affinity to cancerous 5637 cells compared to healthy bladder cells.

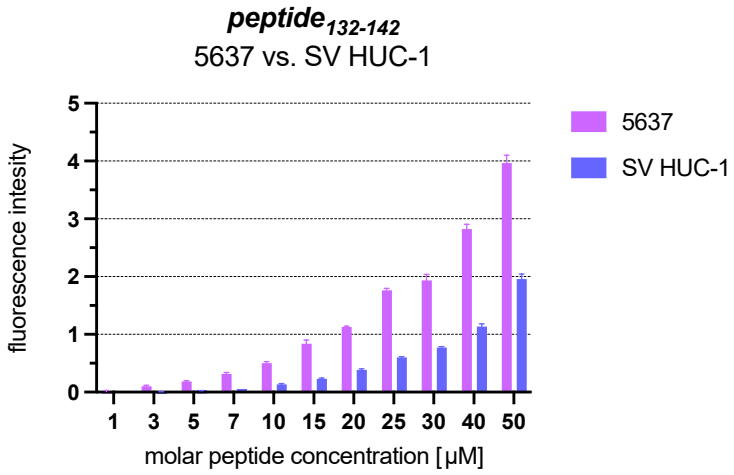

Figure 13: Comparison of cell surface affinity of peptide$_{132-142}$ from 1 µM to 50 µM on 5637 and SV HUC-1 single cells, respectively

The fluorescence intensity signal directly correlates with the cytoadhesive properties of the peptide. Peptide$_{132-142}$ showed a higher fluorescence intensity at all tested concentrations on 5637 single cells compared to SV HUC-1 cells. The data show the mean ± standard deviation in n=3 experiments. All graphs were created with GraphPad Prism.

A possible explanation for the increased affinity to the cancer cells might be an altered protein glycosylation pattern on the cell membrane which plays a role in metastasis and cancer progression. (27, 28) Various cancers are characterized by an altered high mannose type glycosylation. (29) Furthermore, it was found that mannosylation of proteins is overexpressed in bladder cancer cells compared to normal uroepithelial cells. It was also shown that mannose-sensitive type 1 fimbria of UPEC exhibited a higher attachment to bladder cancer cells compared to normal bladder cells. (30) Therefore, the higher affinity of peptide$_{45-55}$ and peptide$_{132-142}$ to cancer bladder cells compared to normal bladder cells aligns with the findings in the referenced studies.

3.6.4 Peptide$_{45-55}$ vs. Peptide$_{132-142}$

To further investigate the binding capacity of the synthesized peptides to cancerous and healthy bladder cells, the mean measured fluorescence intensities of peptide$_{45-55}$ and peptide$_{132-142}$ at different concentrations were directly compared to each other on 5637 and SV HUC-1 single cells, respectively (see figure 14).

On 5637 single cells peptide$_{45-55}$ exhibited a higher cell-bound fluorescence from 3 µM to 40 µM in comparison to peptide$_{132-142}$. At 1 µM and 50 µM peptide$_{132-142}$ showed a slightly higher fluorescence intensity compared to peptide$_{45-55}$ (3.83 ± 0.107 compared to 3.97 ± 0.136 at 50 µM). More precisely, at 40 µM a 30 % higher affinity of peptide$_{45-55}$ to 5637 cells compared to peptide$_{132-142}$ could be measured. At a higher peptide concentration (50 µM) only a 4% difference between the tested peptides on cancerous cells could be observed (see Figure 14a). However, considering the calculated p-values the mean fluorescence intensity differences showed only a statistical significance at 10, 15, 20, 30, and 40 µM (****, p-value < 0.0001) and at 25 µM (*, p-value 0.0329). In the remaining tested concentrations, the results were not considered statistically significant.

On SV HUC-1 single cells a higher cell-associated fluorescence of peptide$_{45-55}$ compared to peptide$_{132-142}$ was measured at all tested concentrations. At the highest concentration (50 µM) peptide$_{45-55}$ showed a 2-fold higher cell-bound fluorescence compared to peptide$_{132-142}$. Additionally, the mean fluorescence difference was statistically significant from 10 to 50 µM (***, p-value < 0.0001) and 7 µM (**, p-value 0.0042) (see Figure 14b).

This indicates that the difference between the investigated peptides regarding the cell adhesion was more pronounced on SV HUC-1 single cells as compared to 5637 cells. Additionally, higher cell-associative properties of peptide$_{45-55}$ could be observed in most of the conducted experiments compared to peptide$_{132-142}$. Considering that peptide$_{132-142}$ comprises one more residue that is part of the carbohydrate-binding pocket of FimH, it is notable that peptide$_{45-55}$ showed superior cell adhesion compared to peptide$_{132-142.}$ (14)

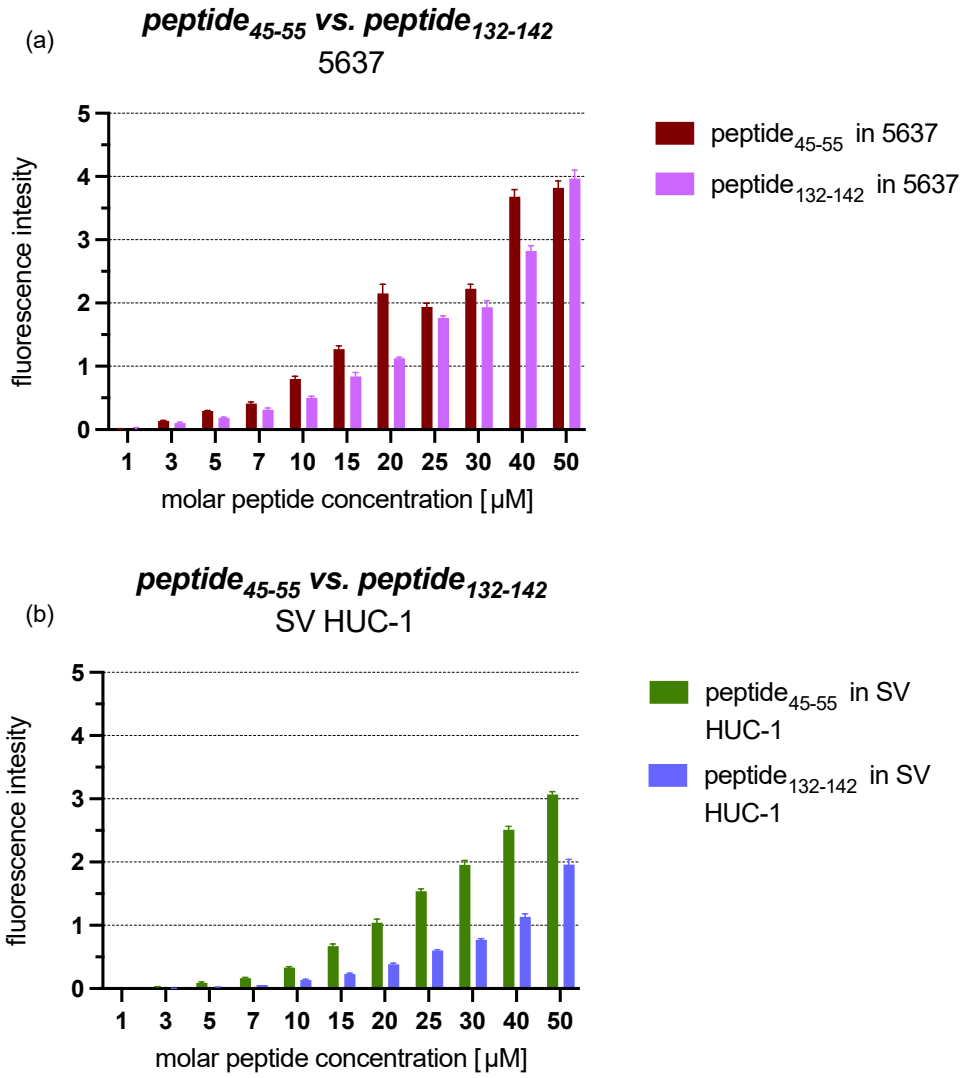

Figure 14: Comparison of cell surface affinity of peptides on 5637 and SV HUC-1 single cells, respectively

The fluorescence intensity directly correlates to the cytoadhesive properties. (a) Cytoadhering of peptide$_{45-55}$ and peptide$_{132-142}$ to 5637 single cells are compared. (b) Cytoadhering of peptide$_{45-55}$ and peptide$_{132-142}$ to SV HUC-1 cells are compared. The data show the mean ± standard deviation of n=3 experiments. All graphs were created with GraphPad Prism.

3.7 Inhibition studies

To investigate the binding specificity of peptide$_{45-55}$ and peptide$_{132-142}$, inhibition assays were performed. Briefly, peptide solutions of 50 µM were prepared which were chosen due to their most significant binding properties in the previous binding studies. Subsequently, the peptide solutions were incubated with different concentrations of α-D-mannose as an inhibitor and α-D-galactose solution as a negative control for 30 minutes. This step was

followed by two additional hours of incubation with the cell suspension at 37 °C (see 2.11 “Inhibition studies”).

The main purpose of this experiment was to identify if the peptides incubated with α-D-mannose or α-D-galactose had a decreased cell surface binding due to saturation of the binding spots. Figure 15 illustrates the mean measured fluorescence intensity of three replicate batches of peptide$_{45\text{-}55}$, peptide$_{132\text{-}142}$ and their corresponding control peptides on 5637 and SV HUC-1 single cells after incubation with different concentrations of α-D-mannose and α-D-galactose, respectively.

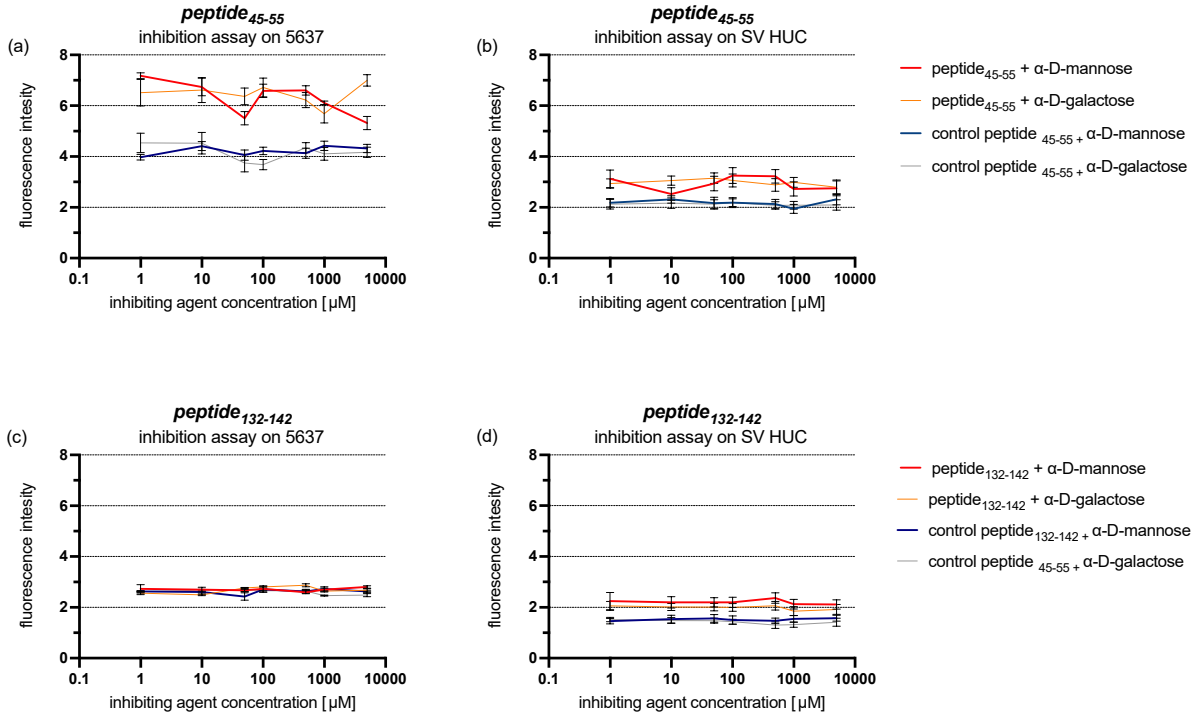

Figure 15: inhibition assay with α-D-mannose and α -D-galactose as a negative control, respectively.

(a) mean measured fluorescence intensity of peptide$_{45\text{-}55}$ and its control peptide$_{45\text{-}55}$ after incubation with different concentrations of α-D-mannose and α-D-galactose, respectively, on 5637 single cells. (b) mean measured fluorescence intensity of peptide$_{45\text{-}55}$ and its control peptide$_{45\text{-}55}$ after incubation with different concentrations of α-D-mannose and α-D-galactose, respectively, on SV HUC-1 single cells. (c) mean measured fluorescence intensity of peptide$_{132\text{-}142}$ and its control peptide$_{132\text{-}142}$ after incubation with different concentrations of α-D-mannose and α-D-galactose, respectively, on 5637 single cells. (d) mean measured fluorescence intensity of peptide$_{132\text{-}142}$ and its control peptide$_{132\text{-}142}$ after incubation with different concentrations of α-D-mannose and α-D-galactose, respectively, on SV HUC-1 single cells. The data show the mean ± standard deviation of n=3 experiments. All graphs were created with GraphPad Prism.

No inhibition with α-D-mannose was determined (see Figure 15).

The experimental setup, however, could provide a potential explanation for these results. Firstly, too low concentrations of the inhibiting agent α-D-mannose could have attributed to the absence of the inhibition. An increased concentration of α-D-mannose might have beneficial effects on the inhibition potency of the sugar molecule. Secondly, the chosen inhibitor α-D-mannose could have been too low in its inhibition potency. It might be possible that other inhibitors that are known as FimH antagonists such as α-methyl mannose (13) may have more potential for an inhibition than α-D-mannose. Moreover, when developing an assay to test adhesion inhibition it must be considered that the results are very dependent on the assay setup. FimH or in the case of this study, the peptides with FimH sequences can either interact with the cell surface or the inhibitor α-D-mannose. Additionally, the inhibitor can also interact with the cell surface. Thus, changes in the experimental setup can have an impact on the results due to altered conditions. (13) Therefore, it might be interesting to investigate the adhesion inhibition in a different experimental setup in which single cells are pre-incubated with the inhibitor before adding the peptide solution.

On the other hand, these results could also suggest that $peptide_{45\text{-}55}$ and $peptide_{132\text{-}142}$ and their control peptides do not bind to the cell surface via α-D-mannose. Nevertheless, additional research is needed to better understand the mechanisms of the underlying binding process between the peptides and the cell surface.

3.8 Fluorescence microscopic analysis

To visualize the cell adhesion and distinguish between surface binding and possible internalization of the peptides, fluorescence microscopic analysis was performed on 5637 monolayers. As described above (see 2.12 “Fluorescence microscopic analysis”) cell monolayers were incubated with 50 µM solutions of $peptide_{45\text{-}55}$, $peptide_{132\text{-}142,}$ and their corresponding control peptides. To trigger potential cytoinvasion of the peptides by active transport mechanisms incubation was performed at 37 °C. To distinguish the cell structures from the investigated peptides, the cell membrane and the nucleus were stained with red fluorescent Alexa-WGA and blue, fluorescent HOECHST 33342, respectively. Figures 16 and 17 show images of all four peptides incubated with 5637 monolayers.

After incubation with the 5637 monolayers all four peptides appeared as green-stained structures around the blue-stained cell nucleus and within the red-stained cell membrane. Furthermore, some green structures were also scattered around the perimeters of the red cell membrane (see Figures 16 and 17). These findings suggest that all investigated peptides exhibited not only cytoadhesive but also cytoinvasive properties.

Subjectively, peptide$_{132\text{-}142}$ and its control peptide$_{132\text{-}142}$ showed similar cytoadhesive and cytoinvasive properties. These results are in line with the data observed in the binding studies (see Figure 11a) where both peptides showed similar binding properties on 5637 cells at 37 °C.

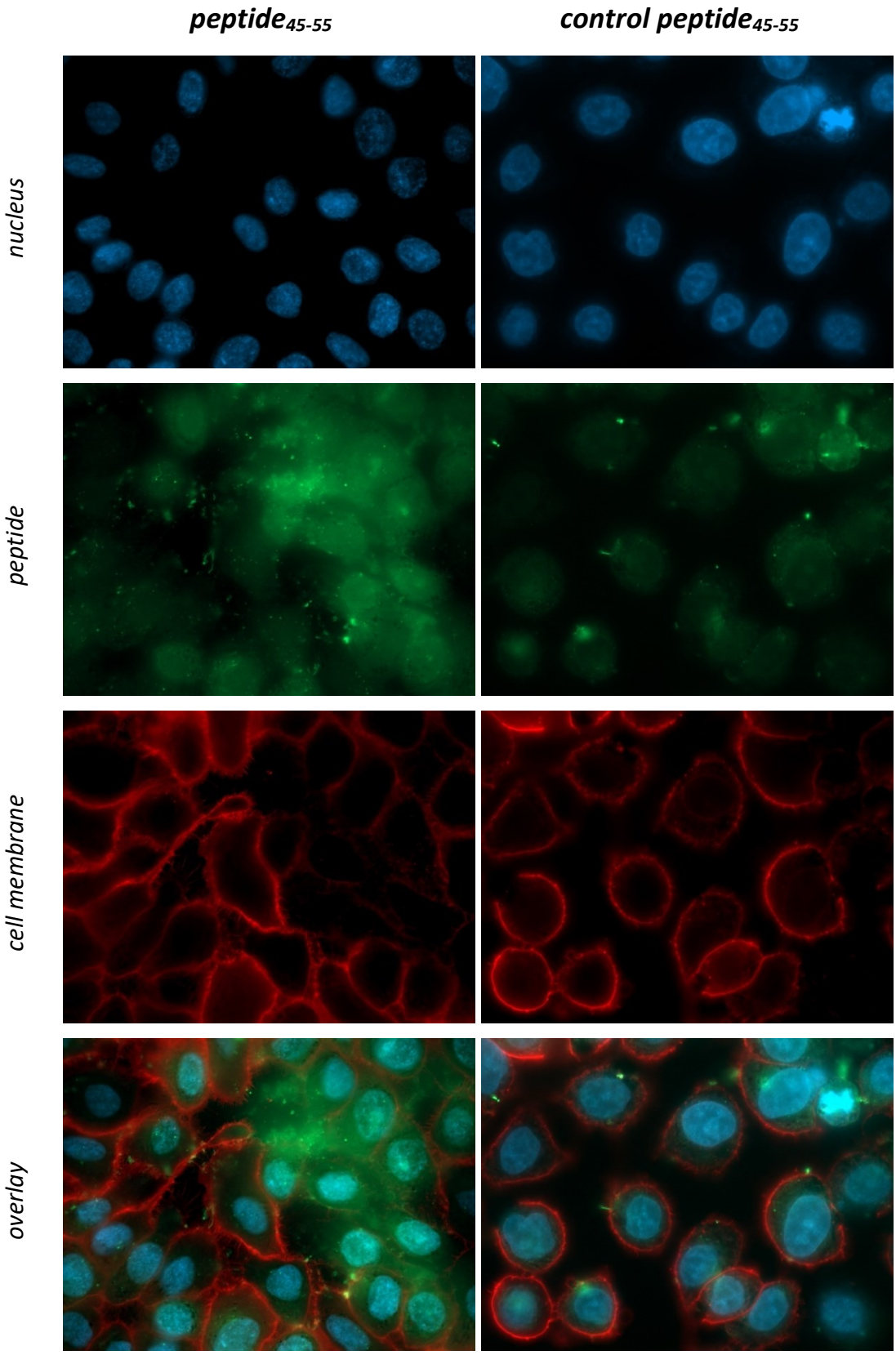

Figure 16: fluorescence microscopic analysis of peptide$_{45-55}$ and its control peptide$_{45-55}$ on 5637 cells at 37 °C

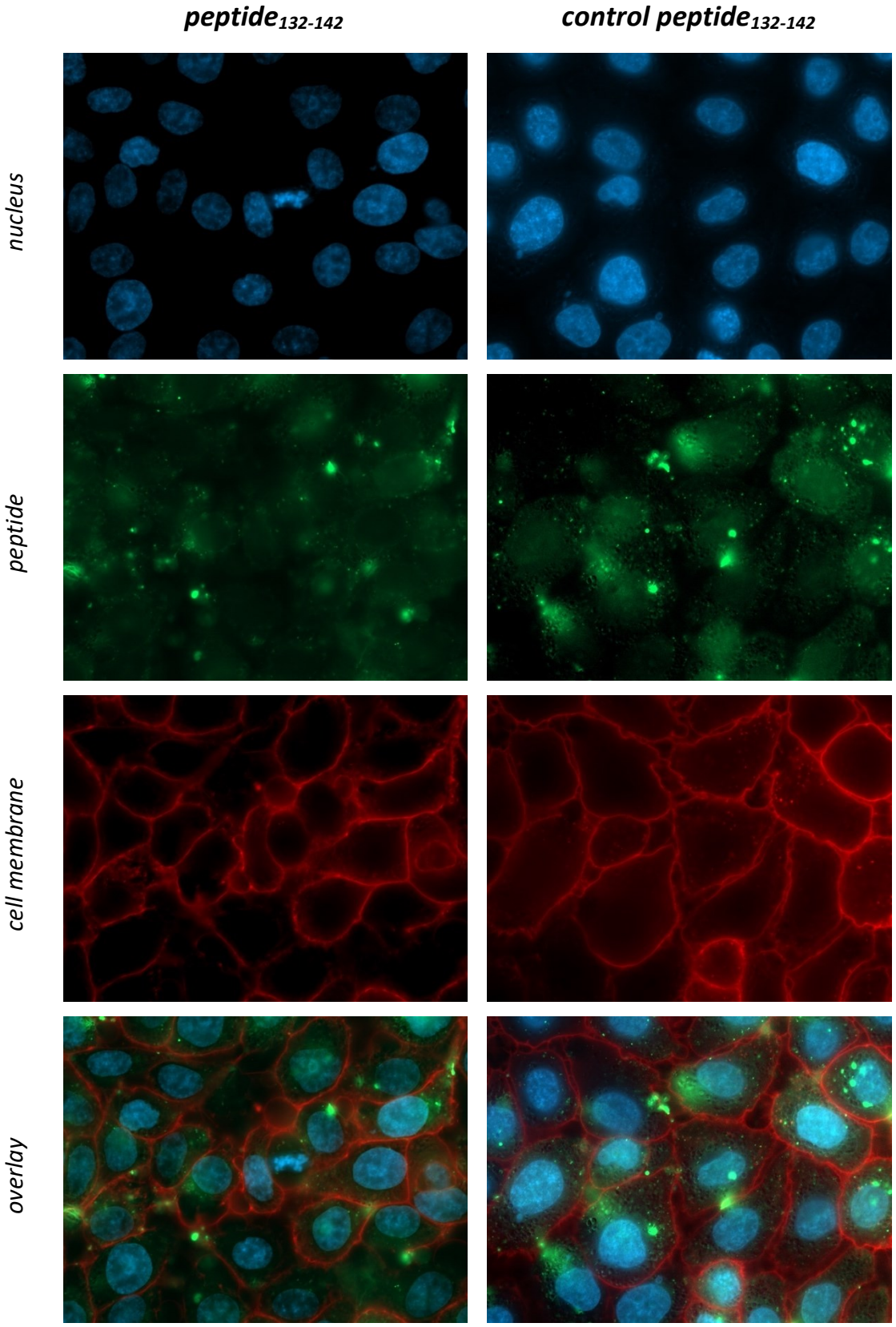

Figure 17: fluorescence microscopic analysis of peptide$_{132-142}$ and its control peptide$_{132-142}$ on 5637 cells at 37 °C

4 Conclusion

Bladder cancer and urinary tract infections are severe conditions affecting the urinary bladder. As they frequently exhibit reoccurrences their treatment is often challenging. Treating bladder diseases with systemically administered drugs presents drawbacks such as limited drug delivery to the affected site, disruption of the host microbiome, and an increased risk of developing drug resistance. To enhance drug delivery to the affected area, direct instillation into the bladder cavity is considered an alternative route as compared to systematic administration. However, direct instillation into the bladder also has several limitations such as drug dilution by the constant urine production and the unique rigid barrier function of the urothelium.

To overcome these limitations this master thesis deals with the characterization of newly designed targeting peptides that contain sequences of the carbohydrate-binding pocket of the bacterial lectin FimH.

Peptide$_{1\text{-}10}$, $_{45\text{-}55}$, $_{132\text{-}142,}$ and their corresponding control peptides were successfully synthesized and characterized in detail. To confirm the cell-adhesive and cytoinvasive properties, cell studies with healthy and cancerous bladder cells were conducted. Peptide$_{45\text{-}55}$ showed superior cell binding properties as compared to its control peptide$_{45\text{-}55}$ to both cancerous and healthy bladder cells. Peptide$_{132\text{-}142}$ showed superior binding compared to its control peptide$_{132\text{-}142}$ for cancerous 5637 cells but not for SV-HUC-1 cells. Furthermore, both peptide$_{45\text{-}55}$ and peptide$_{132\text{-}142}$ showed higher affinity to cancerous 5637 single cells than to SV HUC-1 cells. Additionally, it was observed that peptide$_{45\text{-}55}$ generally showed higher cell-associative potential than peptide$_{132\text{-}142}$ to healthy and cancerous cells. Lastly, it could be demonstrated via fluorescence microscopic analysis that peptide$_{45\text{-}55}$, peptide$_{132\text{-}142,}$ and their respective control peptides exhibited not only cell adhesive properties but were also internalized by bladder cancer cells.

The present study was limited by the absence of peptide$_{1\text{-}10}$ in the cell assays due to unsuccessful purification and quantification. However, it must be noted that peptide$_{1\text{-}10}$ only contained the amino residue Phe1 of the carbohydrate-binding pocket, whereas peptide$_{45\text{-}55}$ and peptide$_{132\text{-}142}$ contained five and six residues, respectively, lining the binding pocket. Nonetheless, a combination of all three peptides via linker molecules should be investigated

in a further study to examine potential synergistic effects and allow the inclusion of peptide $_{1\text{-}10}$ in cell assays.

Within this master thesis, a first step towards the development of new cell-adhesive and cytoinvasive targeting ligands has been taken which hold the potential to substantially improve the instillation therapy for bladder diseases in the foreseeable future.

5 References

1. GuhaSarkar S, Banerjee R. Intravesical drug delivery: challenges, current status, opportunities and novel strategies. Journal of Controlled Release. 2010;148(2):147-59.

2. Bray F, Ferlay J, Soerjomataram I, Siegel RL, Torre LA, Jemal A. Global cancer statistics 2018: GLOBOCAN estimates of incidence and mortality worldwide for 36 cancers in 185 countries. CA Cancer J Clin. 2018;68(6):394-424.

3. Patel VG, Oh WK, Galsky MD. Treatment of muscle-invasive and advanced bladder cancer in 2020. CA: a cancer journal for clinicians. 2020;70(5):404-23.

4. Klein RD, Hultgren SJ. Urinary tract infections: microbial pathogenesis, host–pathogen interactions and new treatment strategies. Nature Reviews Microbiology. 2020;18(4):211-26.

5. Morris CJ, Rohn JL, Glickman S, Mansfield KJ. Effective Treatments of UTI—Is Intravesical Therapy the Future? Pathogens. 2023;12(3):417.

6. Neutsch L, Plattner VE, Polster-Wildhofen S, Zidar A, Chott A, Borchard G, et al. Lectin mediated biorecognition as a novel strategy for targeted delivery to bladder cancer. The Journal of urology. 2011;186(4):1481-8.

7. Apfelthaler C, Anzengruber M, Gabor F, Wirth M. Poly–(l)–glutamic acid drug delivery system for the intravesical therapy of bladder cancer using WGA as targeting moiety. European Journal of Pharmaceutics and Biopharmaceutics. 2017;115:131-9.

8. Brauner B, Schwarz P, Wirth M, Gabor F. Micro vs. nano: PLGA particles loaded with trimethoprim for instillative treatment of urinary tract infections. International Journal of Pharmaceutics. 2020;579:119158.

9. Neutsch L, Wambacher M, Wirth E-M, Spijker S, Kählig H, Wirth M, Gabor F. UPEC biomimickry at the urothelial barrier: lectin-functionalized PLGA microparticles for improved intravesical chemotherapy. International journal of pharmaceutics. 2013;450(1-2):163-76.

10. Skoll K, Palmetzhofer J, Lummerstorfer M, Anzengruber M, Gabor F, Wirth M. Human serum albumin nanoparticles as a versatile vehicle for targeted delivery of antibiotics to combat bacterial infections. Nanomedicine: Nanotechnology, Biology and Medicine. 2023;50:102685.

11. Skoll K, Ritschka M, Fuchs S, Wirth M, Gabor F. Characterization of sonochemically prepared human serum albumin nanocapsules using different plant oils as core component for targeted drug delivery. Ultrasonics Sonochemistry. 2021;76:105617.

12. Ambrosi M, Cameron NR, Davis BG. Lectins: tools for the molecular understanding of the glycocode. Organic & Biomolecular Chemistry. 2005;3(9):1593-608.

13. Hartmann M, Lindhorst TK. The bacterial lectin FimH, a target for drug discovery–carbohydrate inhibitors of type 1 fimbriae-mediated bacterial adhesion. European Journal of Organic Chemistry. 2011;2011(20-21):3583-609.

14. Choudhury D, Thompson A, Stojanoff V, Langermann S, Pinkner J, Hultgren SJ, Knight SD. X-ray structure of the FimC-FimH chaperone-adhesin complex from uropathogenic Escherichia coli. Science. 1999;285(5430):1061-6.

15. Westerlund-Wikström B, Korhonen TK. Molecular structure of adhesin domains in Escherichia coli fimbriae. Int J Med Microbiol. 2005;295(6-7):479-86.

16. Wu XR, Sun TT, Medina JJ. In vitro binding of type 1-fimbriated Escherichia coli to uroplakins Ia and Ib: relation to urinary tract infections. Proc Natl Acad Sci U S A. 1996;93(18):9630-5.

17. Mulvey MA, Lopez-Boado YS, Wilson CL, Roth R, Parks WC, Heuser J, Hultgren SJ. Induction and evasion of host defenses by type 1-piliated uropathogenic Escherichia coli. Science. 1998;282(5393):1494-7.

18. Hung CS, Bouckaert J, Hung D, Pinkner J, Widberg C, DeFusco A, et al. Structural basis of tropism of Escherichia coli to the bladder during urinary tract infection. Mol Microbiol. 2002;44(4):903-15.

19. Chan W, Peter W. Fmoc Solid Phase Peptide Synthesis : A Practical Approach. New York: OUP Oxford; 2000.

20. Manne SR, Sharma A, Sazonovas A, El-Faham A, de la Torre BG, Albericio F. Understanding OxymaPure as a Peptide Coupling Additive: A Guide to New Oxyma Derivatives. ACS Omega. 2022;7(7):6007-23.

21. [cited 2023 30.08.2023]. Available from: https://www.rapp-polymere.com/index.php?id=725.

22. Ste Marie EJ, Hondal RJ. Reduction of cysteine-S-protecting groups by triisopropylsilane. J Pept Sci. 2018;24(11):e3130.

23. Scientific T. Tech Tip #6 Extinction Coefficients 2013 [Available from: https://assets.thermofisher.com/TFS-Assets/LSG/Application-Notes/TR0006-Extinction-coefficients.pdf.

24. Gill SC, Von Hippel PH. Calculation of protein extinction coefficients from amino acid sequence data. Analytical biochemistry. 1989;182(2):319-26.

25. Scientific T. Tech Tip #31 Calculate dye:protein (F/P) molar ratios 2011 [Available from: https://assets.thermofisher.com/TFS-Assets/LSG/brochures/TR0031-Calc-FP-ratios.pdf.

26. Scharenberg M, Abgottspon D, Cicek E, Jiang X, Schwardt O, Rabbani S, Ernst B. A flow cytometry-based assay for screening FimH antagonists. Assay Drug Dev Technol. 2011;9(5):455-64.

27. Oh YJ, Dent MW, Freels AR, Zhou Q, Lebrilla CB, Merchant ML, Matoba N. Antitumor activity of a lectibody targeting cancer-associated high-mannose glycans. Molecular Therapy. 2022;30(4):1523-35.

28. Oliveira-Ferrer L, Legler K, Milde-Langosch K, editors. Role of protein glycosylation in cancer metastasis. Seminars in cancer biology; 2017: Elsevier.

29. Loke I, Kolarich D, Packer NH, Thaysen-Andersen M. Emerging roles of protein mannosylation in inflammation and infection. Molecular aspects of medicine. 2016;51:31-55.

30. Maalouf N, Gur C, Yutkin V, Scaiewicz V, Mandelboim O, Bachrach G. High mannose level in bladder cancer enhances type 1 fimbria–mediated attachment of uropathogenic E. coli. Frontiers in Cellular and Infection Microbiology. 2022;12:968739.

6 Table of Figures

Appendix

Appendix 1: Complete listing of the used Fmoc-protected amino acids

- Fmoc-L-Ala-OH*H2O
- Fmoc-L-Arg(Pbf)-OH
- Fmoc-L-Asn(Trt)-OH
- Fmoc-L-Asp(OtBu)-OH
- Fmoc-L-Cys(Trt)-OH
- Fmoc-L-Gln(Trt)-OH
- Fmoc-L-Glu(OtBu)-OH*H2o
- Fmoc-L-His(Trt)-OH
- Fmoc-L-Ile-OH
- Fmoc-L-Lys(Dde)-OH
- Fmoc-L-Phe-OH
- Fmoc-L-Pro-OH*H2O
- Fmoc-L-Ser(tBu)-OH
- Fmoc-L-Tyr(tBu)-OH
- Fmos-L-Lys(Boc)-OH

Appendix 2: Preparative HPLC chromatograms

Preparative HPLC peptide$_{1\text{-}10}$

Column: PREPURE 250x10
Flow Rate: 5 mL/min
Equilibration: 2.0 min
Run Length: 30.0 min
Instrument Type: C-850
Mode: Prep
Sample type: Liquid

Solvent A: Water + 0.1% TFA
Solvent B: Acetonitrile + 0.1% TFA
Solvent C: Empty
Solvent D: Empty
Slope Detection: Off

UV Threshold: 0.05 AU
UV Sensitivity: High
UV1 λ: 214 nm
UV2 λ: 280 nm
UV3 λ: 440 nm
UV4 λ: N/A
UV scan start λ: 200 nm (M)
UV scan end λ: 500 nm (M)

ELSD Threshold: N/A
ELSD Sensitivity: Low
Collection: Collect Peaks
Per-Vial Volume: 25 mL
Non-Peak Volume: 25 mL

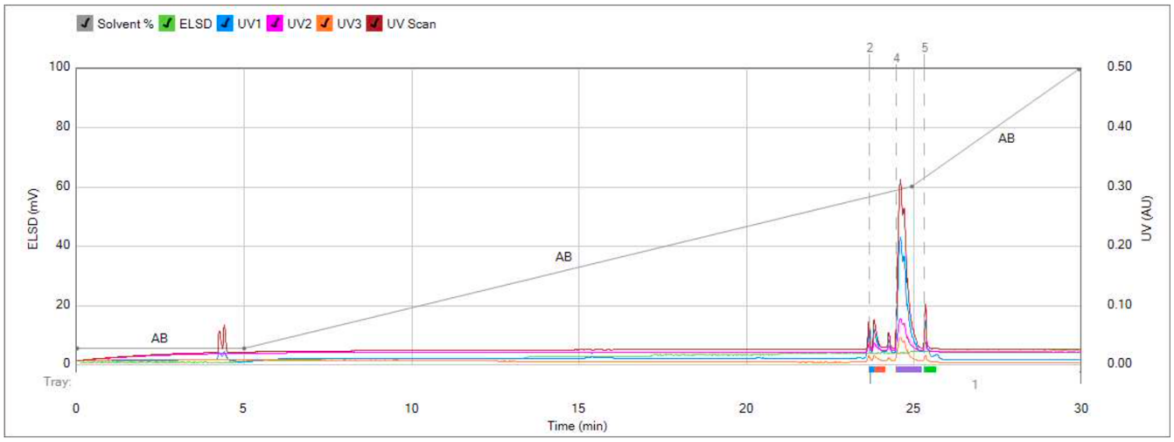

Preparative HPLC control peptide$_{1\text{-}10}$

Not available

Preparative HPLC peptide$_{45\text{-}55}$

Column: PrepPure C18 250x10
Flow Rate: 5 mL/min
Equilibration: 2.0 min
Run Length: 25.0 min
Instrument Type: C-850
Mode: Prep
Sample type: Liquid

Solvent A: Water + 0.1% TFA
Solvent B: Acetonitrile + 0.1% TFA
Solvent C: Empty
Solvent D: Empty
Slope Detection: Off

UV Threshold: 0.05 AU
UV Sensitivity: High
UV1 λ: 214 nm
UV2 λ: 280 nm
UV3 λ: 440 nm
UV4 λ: N/A
UV scan start λ: 200 nm (M)
UV scan end λ: 500 nm (M)

ELSD Threshold: N/A
ELSD Sensitivity: Low
Collection: Collect Peaks
Per-Vial Volume: 25 mL
Non-Peak Volume: 25 mL

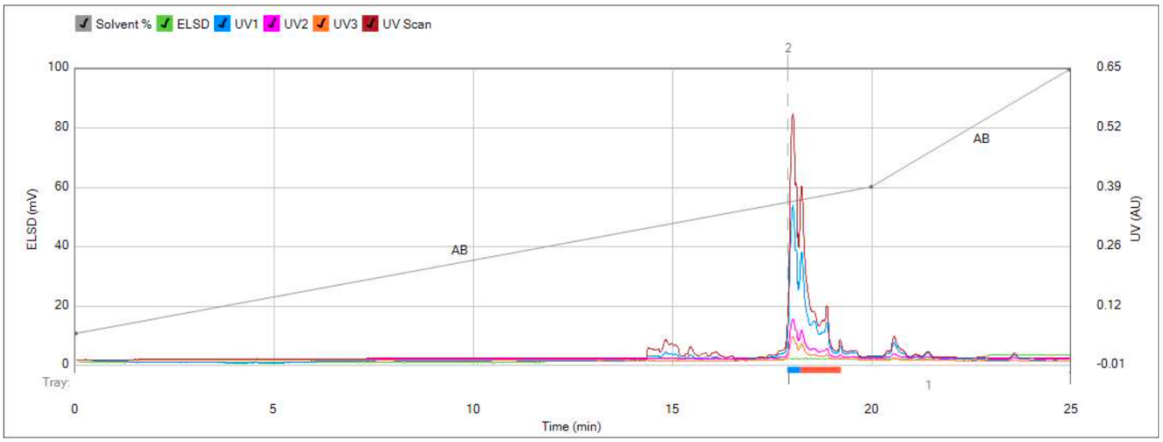

Preparative HPLC control peptide$_{45\text{-}55}$

Column: PP C18
Flow Rate: 5 mL/min
Equilibration: 2.0 min
Run Length: 30.0 min
Instrument Type: C-850
Mode: Prep
Sample type: Liquid

Solvent A: Water + 0.1% TFA
Solvent B: Acetonitrile + 0.1% TFA
Solvent C: Empty
Solvent D: Empty
Slope Detection: Off

UV Threshold: 0.05 AU
UV Sensitivity: High
UV1 λ: 214 nm
UV2 λ: 280 nm
UV3 λ: 440 nm
UV4 λ: 320 nm (M)
UV scan start λ: 200 nm
UV scan end λ: 500 nm

ELSD Threshold: 20 mV
ELSD Sensitivity: Low
Collection: Collect Peaks
Per-Vial Volume: 25 mL
Non-Peak Volume: 25 mL

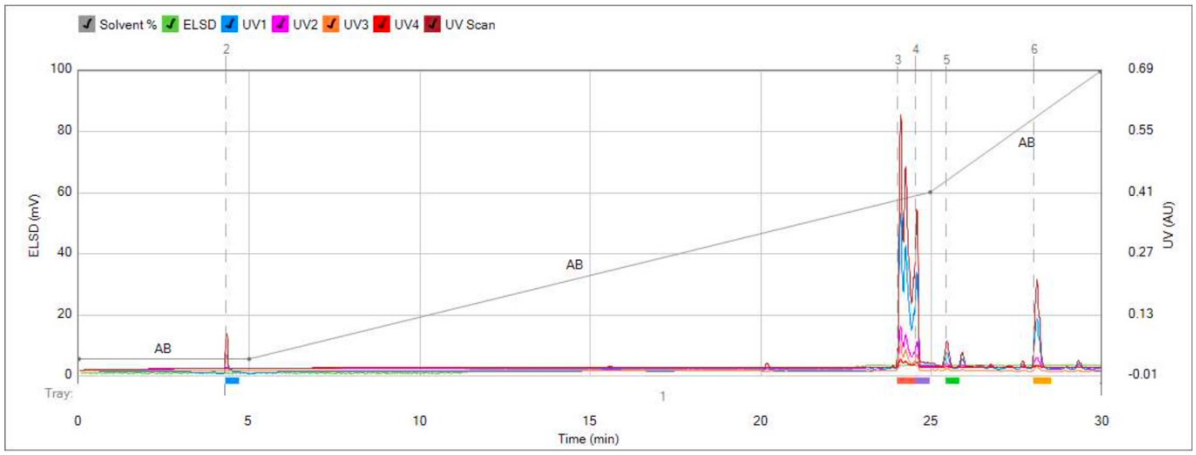

Preparative HPLC peptide$_{132\text{-}142}$

Column: PrepPure C18 250x10
Flow Rate: 5 mL/min
Equilibration: 2.0 min
Run Length: 25.0 min
Instrument Type: C-850
Mode: Prep
Sample type: Liquid

Solvent A: Water + 0.1% TFA
Solvent B: Acetonitrile + 0.1% TFA
Solvent C: Empty
Solvent D: Empty
Slope Detection: Off

UV Threshold: 0.05 AU
UV Sensitivity: High
UV1 λ: 214 nm
UV2 λ: 280 nm
UV3 λ: 440 nm
UV4 λ: N/A
UV scan start λ: 200 nm (M)
UV scan end λ: 500 nm (M)

ELSD Threshold: N/A
ELSD Sensitivity: Low
Collection: Collect Peaks
Per-Vial Volume: 25 mL
Non-Peak Volume: 25 mL

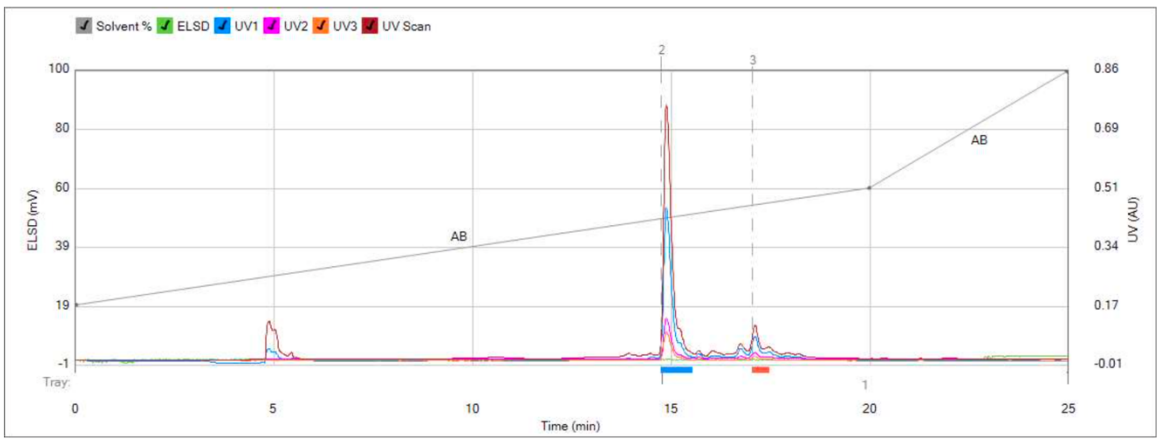

Preparative HPLC control peptide$_{132-142}$

Column: PP C18	Solvent A: Water + 0.1% TFA	UV Threshold: 0.05 AU	ELSD Threshold: 20 mV
Flow Rate: 5 mL/min	Solvent B: Acetonitrile + 0.1% TFA	UV Sensitivity: High	ELSD Sensitivity: Low
Equilibration: 2.0 min	Solvent C: Empty	UV1 λ: 214 nm	Collection: Collect Peaks
Run Length: 30.0 min	Solvent D: Empty	UV2 λ: 280 nm	Per-Vial Volume: 25 mL
Instrument Type: C-850	Slope Detection: Off	UV3 λ: 440 nm	Non-Peak Volume: 25 mL
Mode: Prep		UV4 λ: 320 nm (M)	
Sample type: Liquid		UV scan start λ: 200 nm	
		UV scan end λ: 500 nm	

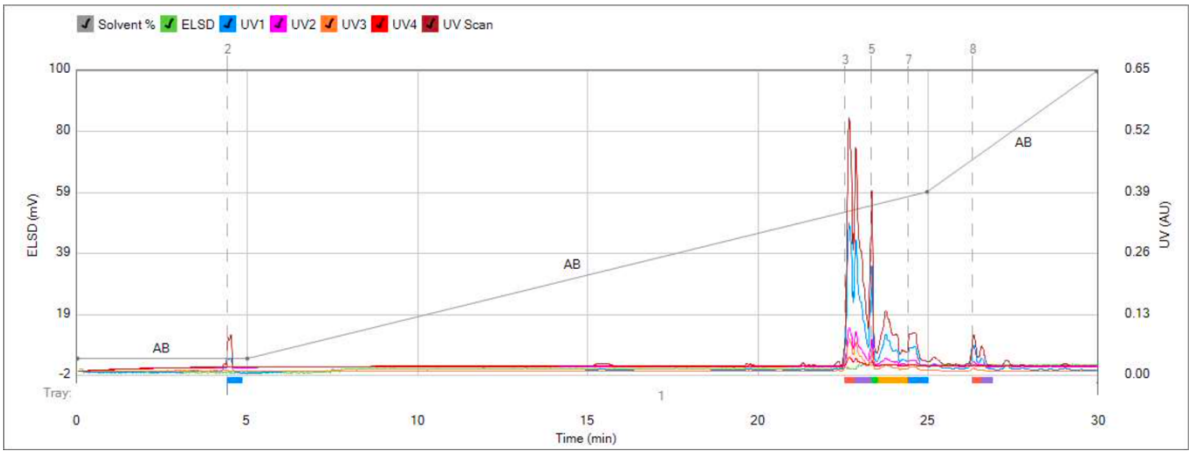

Appendix 3: Analytical HPLC chromatograms

Peptide$_{1-10}$ before purification

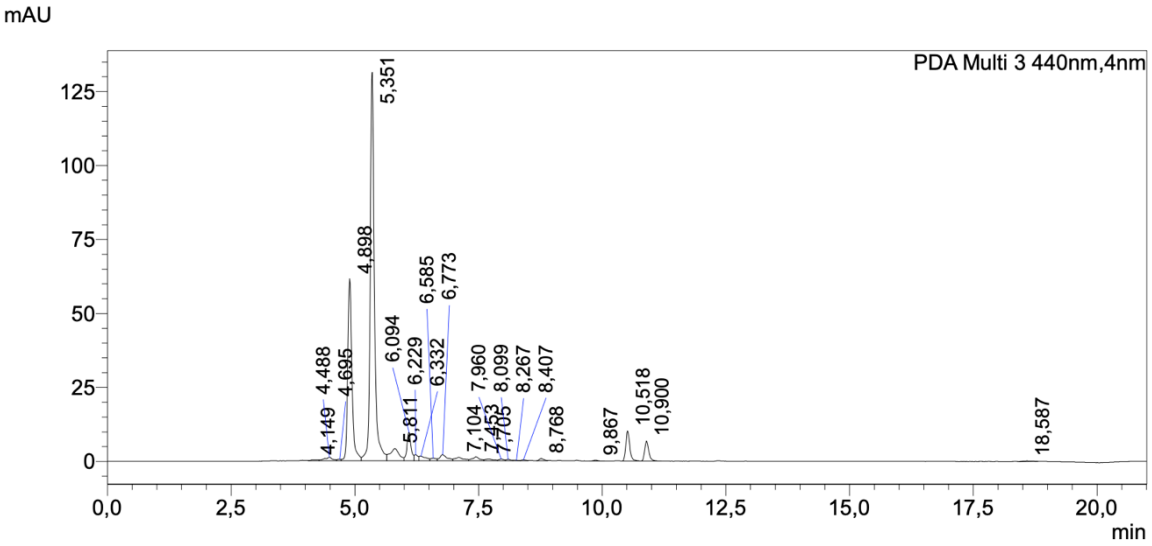

Peptide$_{1-10}$ after purification

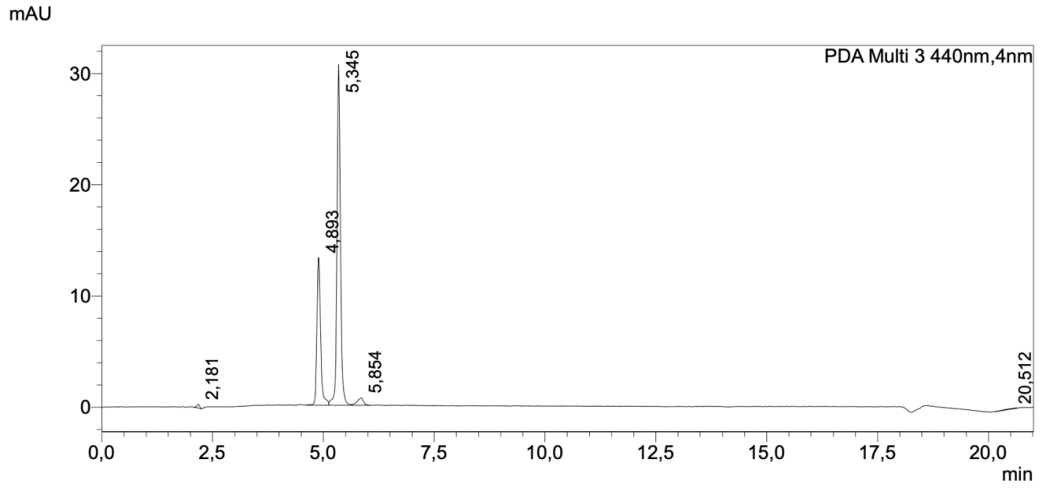

Control peptide$_{1-10}$ before purification

Not available

Control peptide$_{1-10}$ after purification

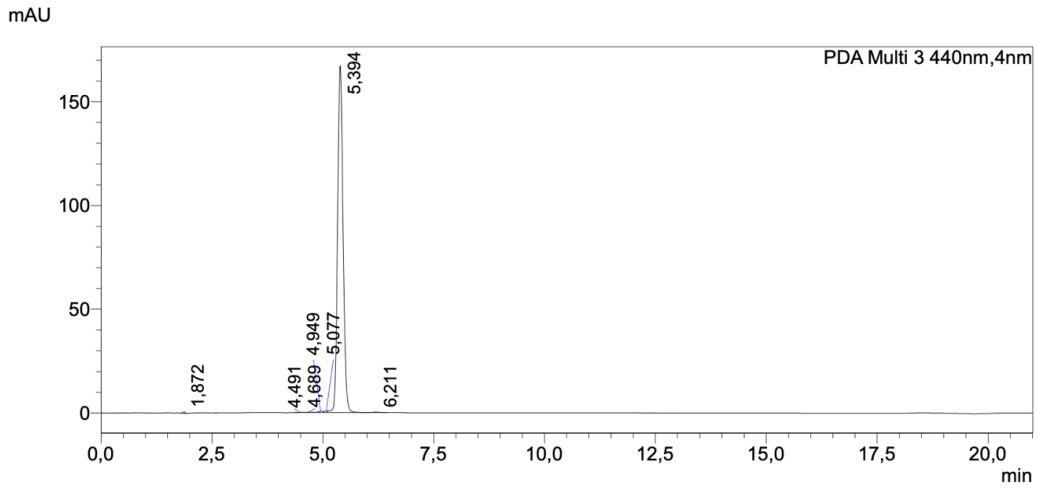

Peptide$_{45-55}$ before purification

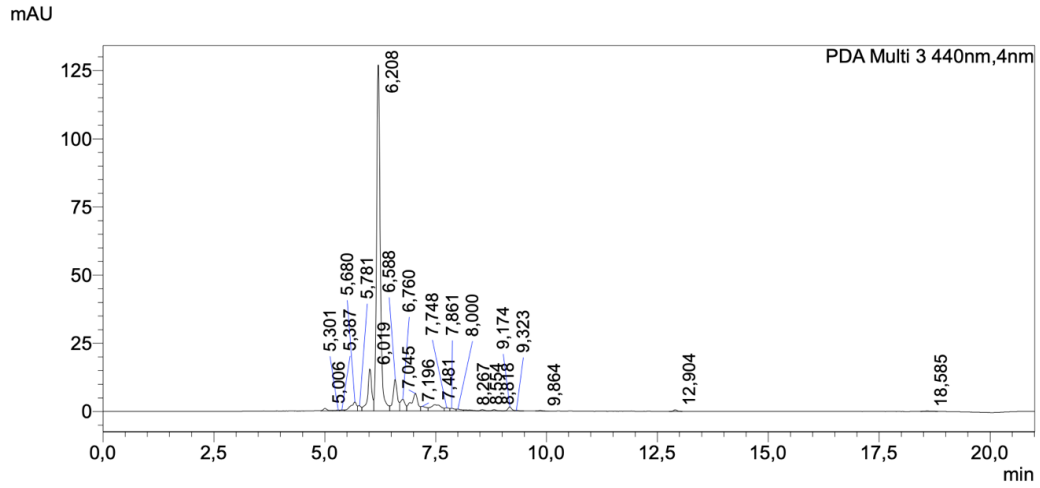

Peptide$_{45-55}$ after purification

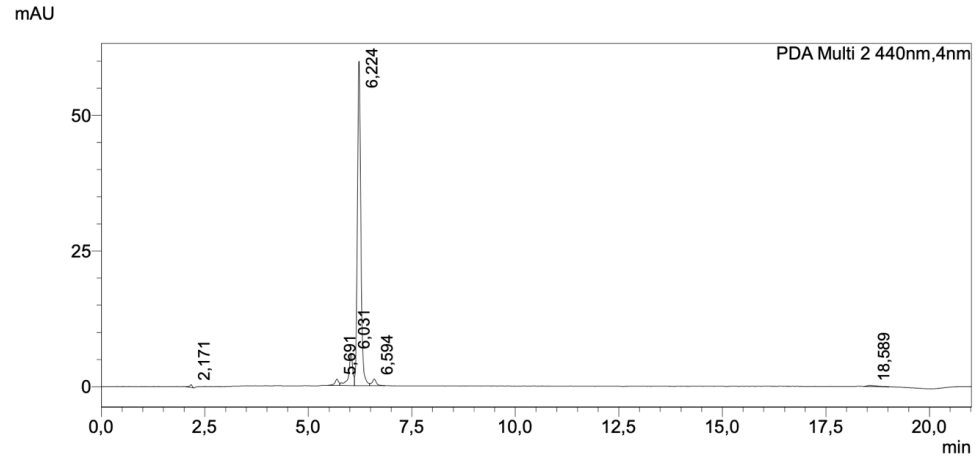

Control peptide$_{45-55}$ before purification

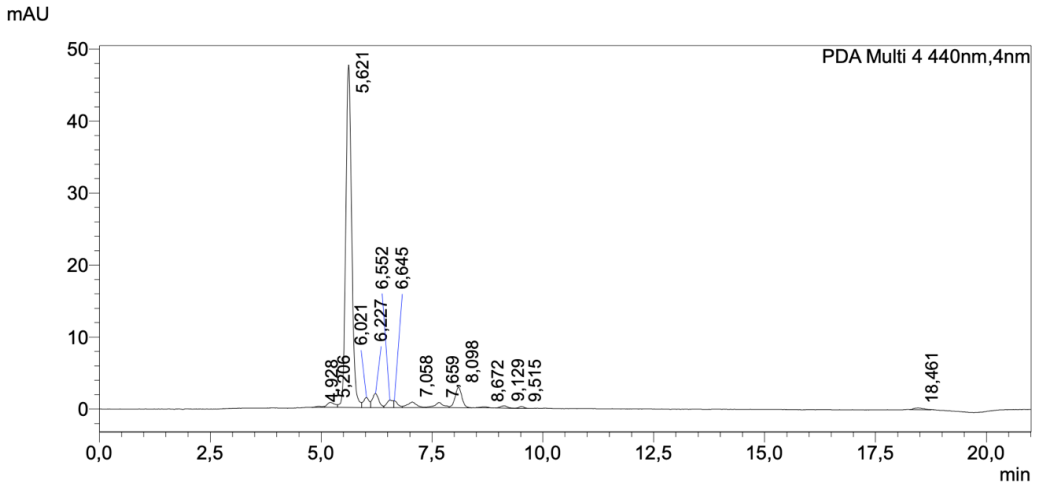

Control peptide$_{45-55}$ after purification

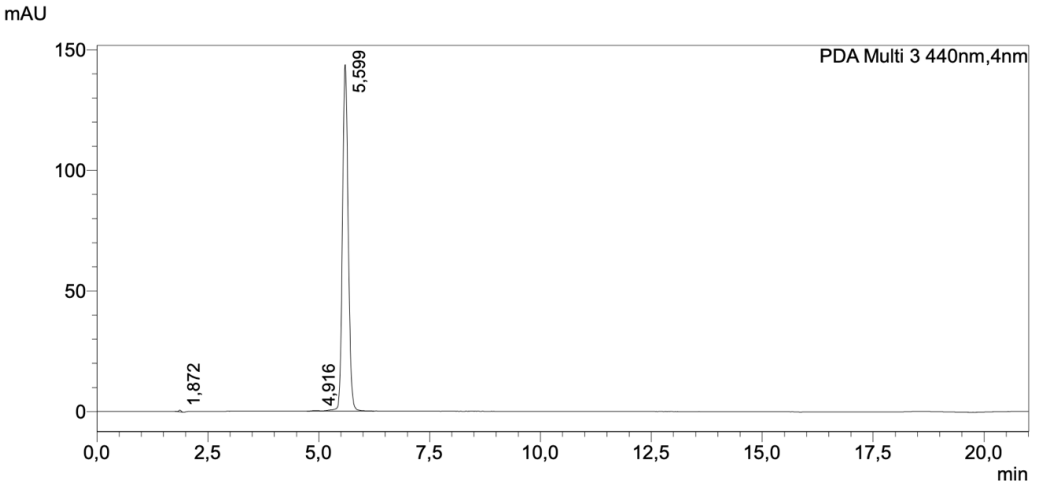

Peptide$_{132\text{-}142}$ before purification

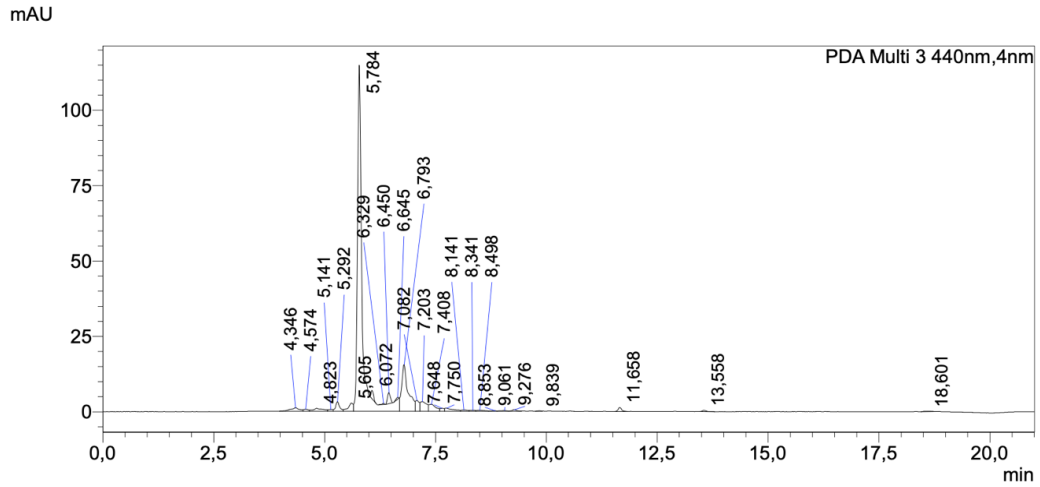

Peptide$_{132\text{-}142}$ after purification

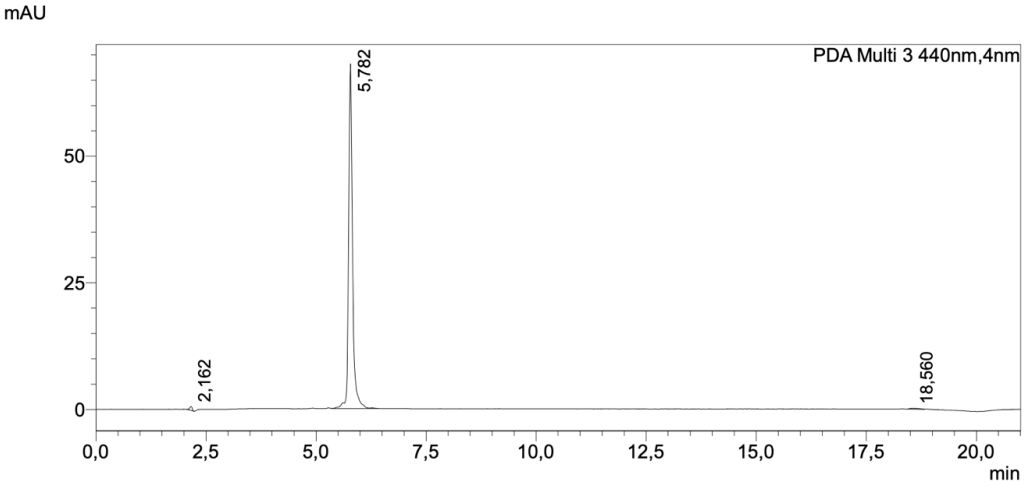

Control peptide$_{132\text{-}142}$ before purification

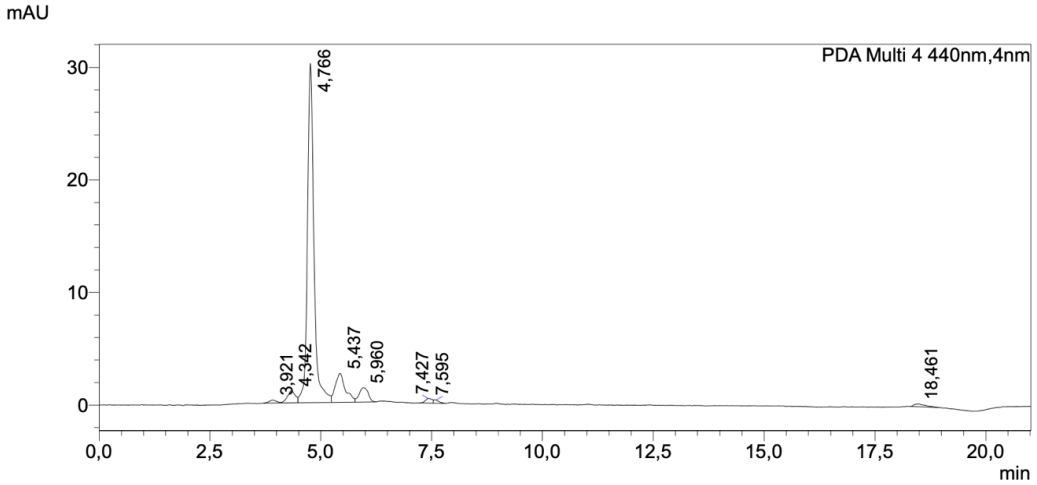

Control peptide$_{132-142}$ after purification

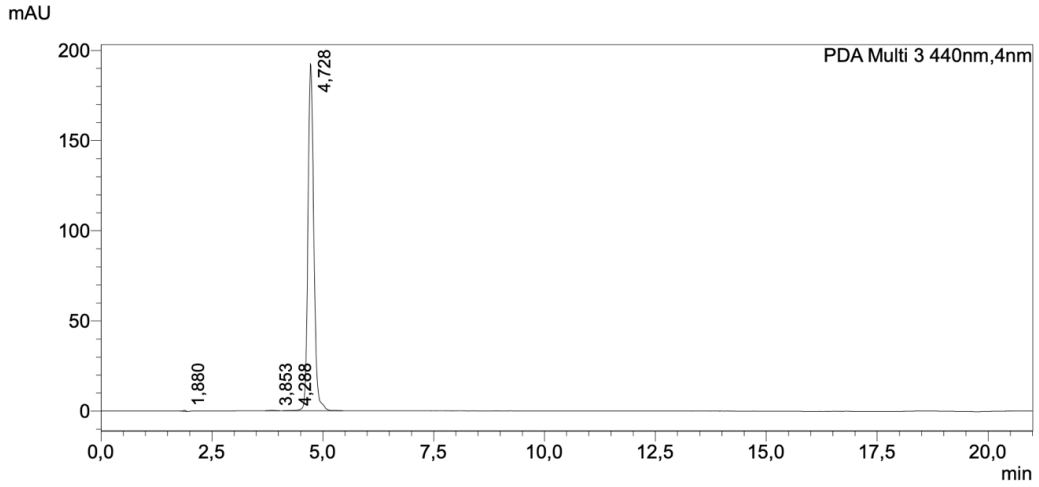

Appendix 4: Mass spectrums

Mass spectrums peptide$_{1\text{-}10}$ and control peptide$_{1\text{-}10}$

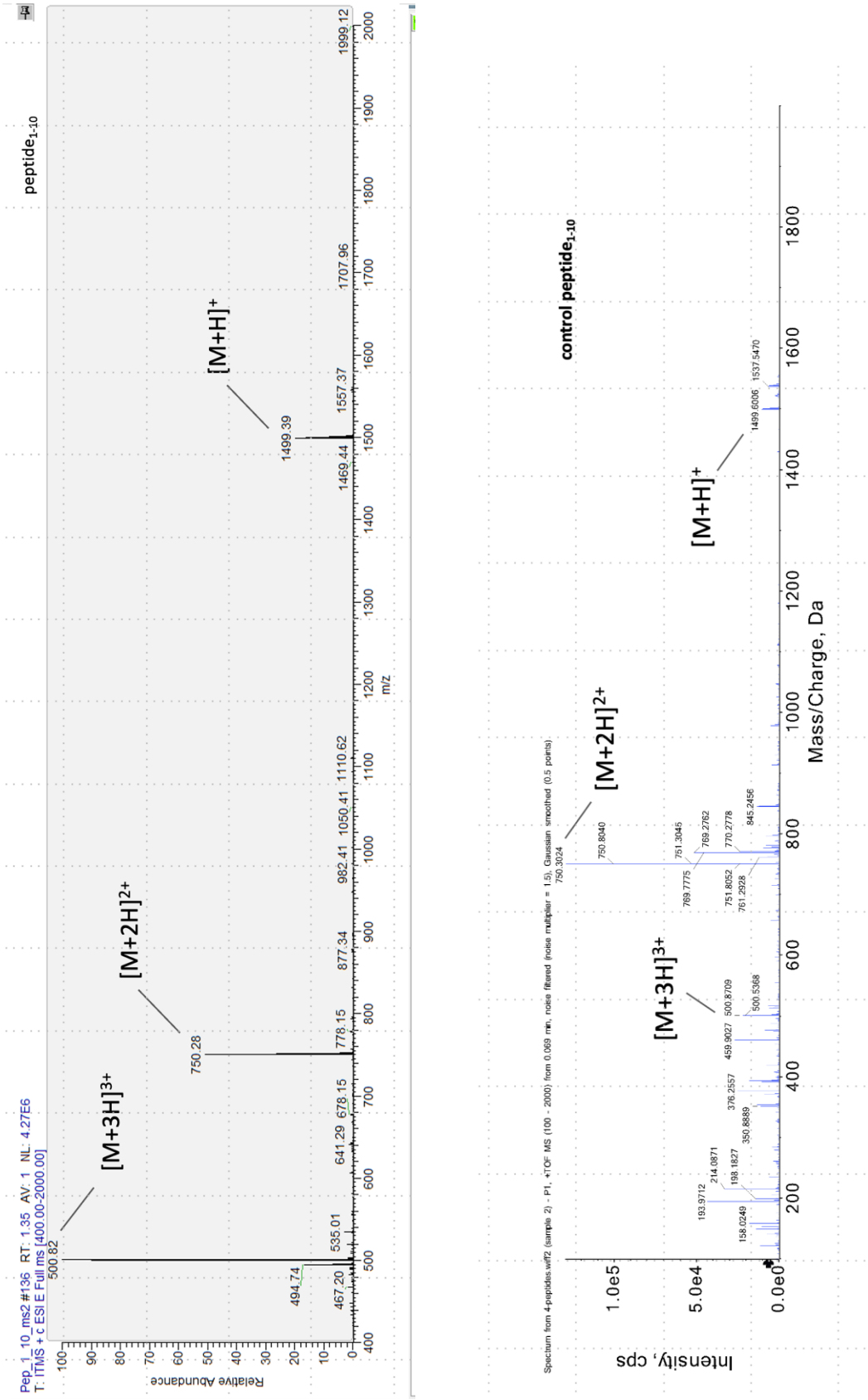

Mass spectrums peptide$_{45\text{-}55}$ and control peptide$_{45\text{-}55}$

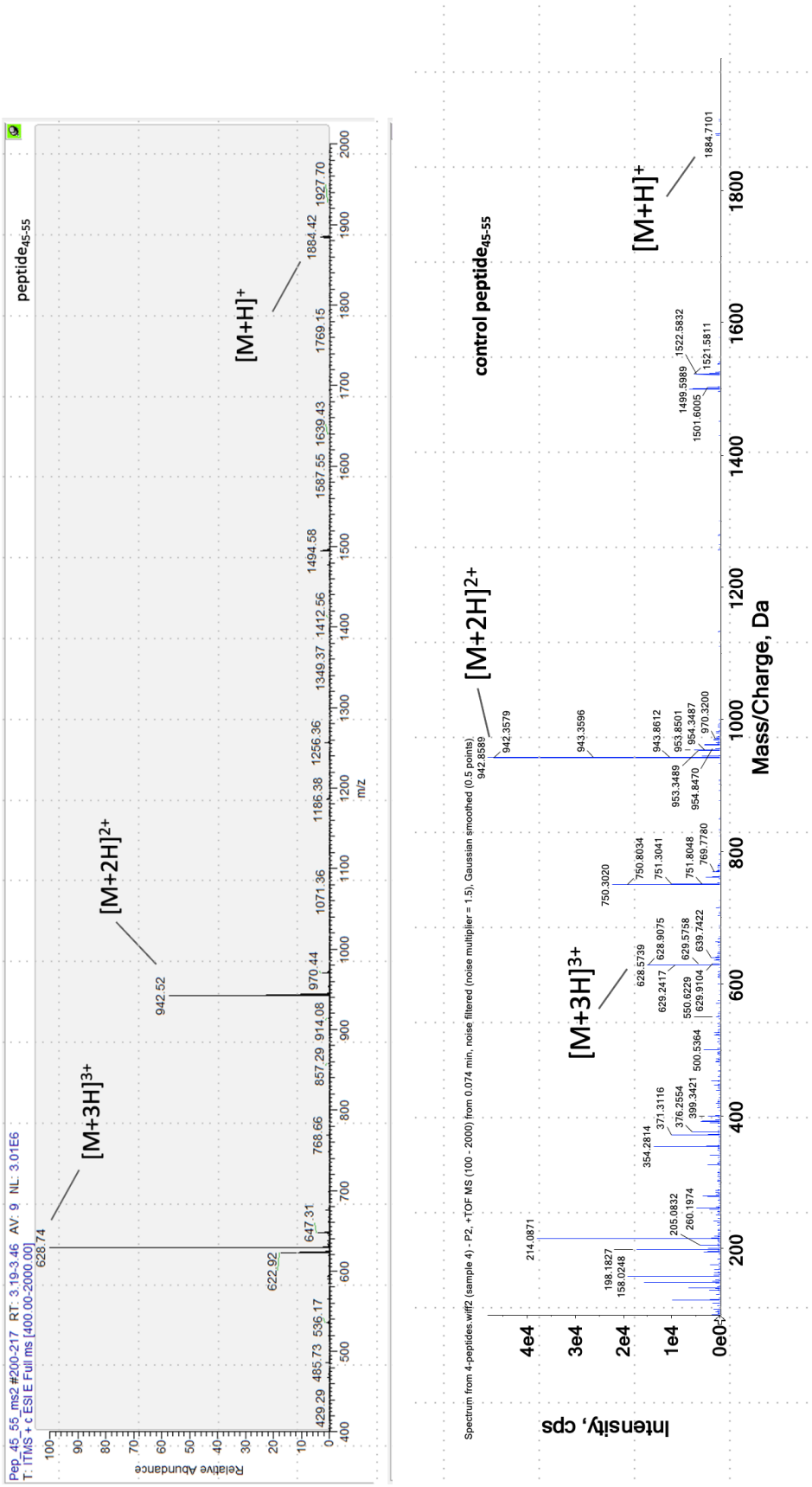

Mass spectrums peptide$_{132-142}$ and control peptide$_{132-142}$

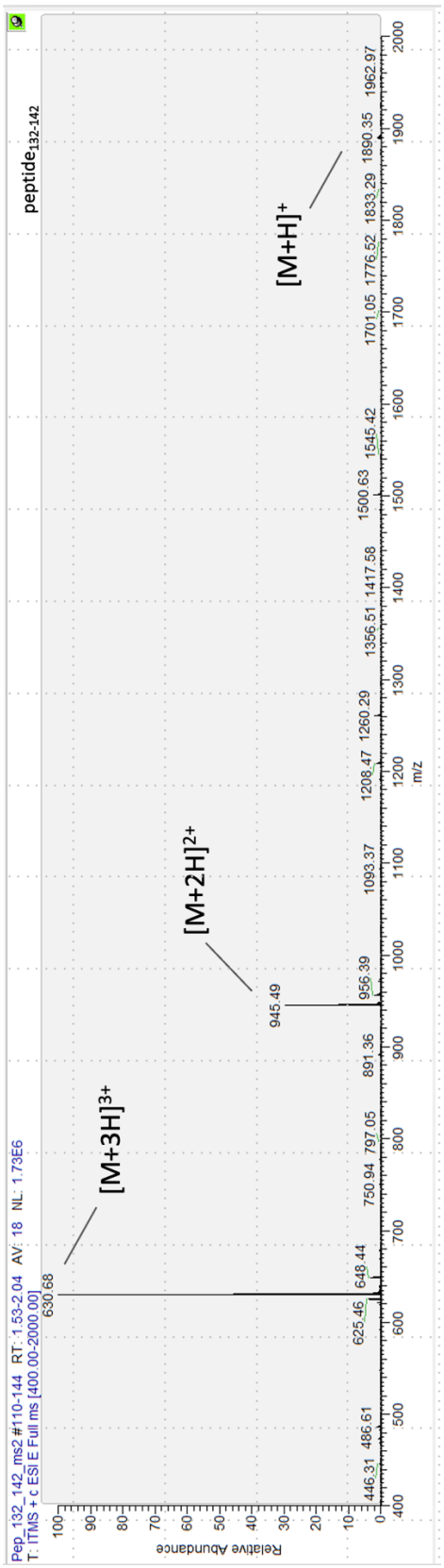

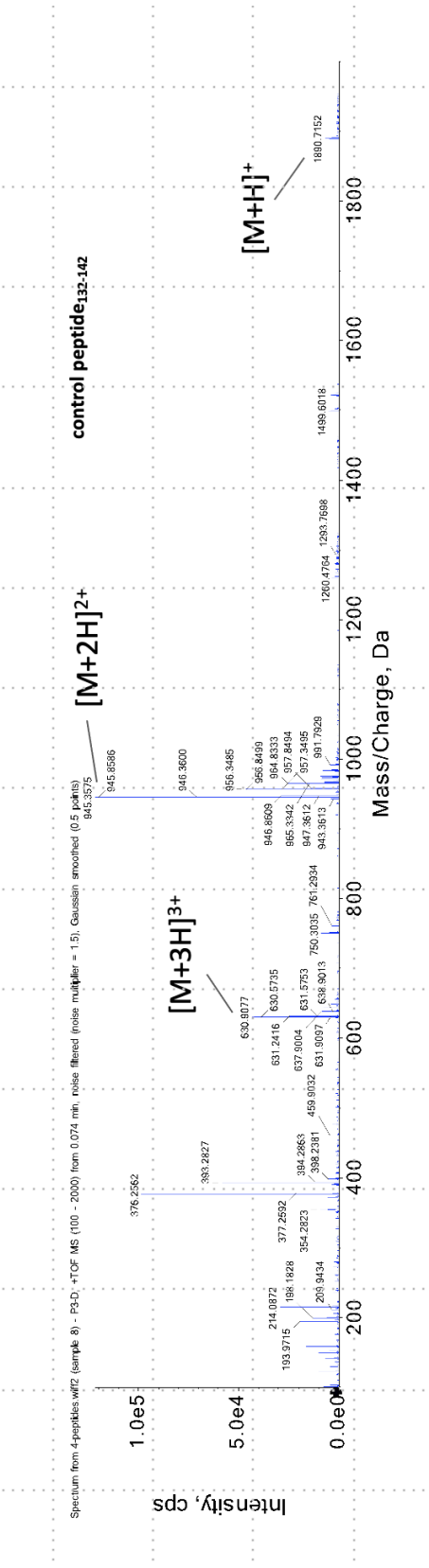

Appendix 5: Zusammenfassung

Die Therapie von Erkrankungen der Harnblase, wie Blasenkarzinome und Harnwegsinfekte, wird häufig durch das Auftreten von Rezidiven erschwert. Eine instillative Therapie ermöglicht zwar die direkte Applikation einer Wirkstofflösung an dem betroffenen Organ, ist aber durch Verdünnungseffekte aufgrund der konstanten Urinproduktion und durch die dichte Barrierefunktion der Harnblase in seiner Effizienz limitiert.

In der vorliegenden Masterarbeit sollten für ein zukünftiges Drug Delivery System Peptide mit einer gezielten Affinität für die Harnblase zu entwickelt werden, um die Verweildauer von Wirkstoffen in der Harnblase nach einer instillativen Therapie zu verlängern. Dafür wurden Peptidanaloga, die bindungsaffine Primärsequenzen des bakteriellen Lektins FimH enthalten, synthetisiert, charakterisiert und auf ihre zelladhäsiven Eigenschaften an gesunden und kanzerösen Blasenzellen untersucht.

Die synthetisierten Peptide zeigten sowohl an gesunden Blasenzellen als auch an Krebsblasenzellen zelladhäsive Eigenschaften, wobei insbesondere an Blasenkarzinomzellen eine deutliche Bindung festgestellt werden konnte. Zudem konnte durch Fluoreszenzmikroskopie gezeigt werden, dass die Peptide nicht nur zelladhäsive Eigenschaften aufweisen, sondern von Blasenkarzinomzellen auch internalisiert werden.

Somit stellen die vorgestellten Peptidanaloga mit Primärsequenzen des Lektins FimH potenzielle Targeting Moleküle dar, die in Zukunft die Limitationen in der instillativen Therapie bei Blasenkrebs und Harnwegsinfekten minimieren könnten.